

INSTRUMENTATION FOR LUNGS SOUND MEASUREMENT

A DISSERTATION

*Submitted in partial fulfillment of the
requirements for the award of the degree*

of

MASTER OF TECHNOLOGY

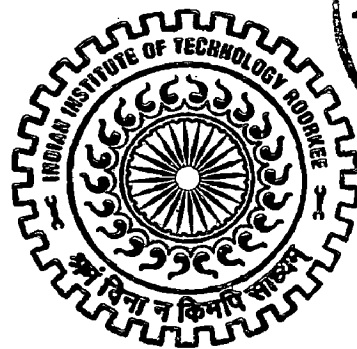
in

ELECTRICAL ENGINEERING

(With Specialization in Measurement & Instrumentation)

By

VENKATA GIRISH POTNURU



**DEPARTMENT OF ELECTRICAL ENGINEERING
INDIAN INSTITUTE OF TECHNOLOGY ROORKEE
ROORKEE-247 667 (INDIA)**

JUNE, 2006



INDIAN INSTITUTE OF TECHNOLOGY
ROORKEE-247667

CANDIDATE'S DECLARATION

I hereby declare that the work, which is being presented in this dissertation entitled "Instrumentation for Lungs Sound Measurement" in the partial fulfillment of the requirement for the award of the degree of **Master of Technology in Electrical Engineering** with specialization in **Measurement and Instrumentation**, submitted in the **Department of Electrical Engineering, Indian Institute of Technology Roorkee, Roorkee**, is an authentic record of my own work carried out during July 2005 to June 2006 under the supervision of **Dr. R.S.Anand**, Associate Professor, Department of Electrical Engineering, Indian Institute of Technology Roorkee, Roorkee.

I have not submitted the matter embodied in this dissertation for award of any other degree.

Date: June 2006

W. Girish
(VENKATA GIRISH POTNURU)

Place: Roorkee

CERTIFICATE

This is to certify that the above statement made by the candidate is true to the best of my knowledge.

Date: *26.06.2006*

Place: Roorkee

Dr. R.S. Anand
26.06.2006
Dr.R.S.Anand

Associate Professor,
Department of Electrical Engineering,
Indian Institute of Technology Roorkee,
Roorkee – 247667.
India

ACKNOWLEDGEMENTS

I express my foremost and deepest gratitude to **Dr.R.S.Anand**, Associate Professor, Department of Electrical Engineering, Indian Institute of Technology Roorkee, Roorkee for his valuable guidance, support and motivation throughout this work. I have deep sense of admiration for his innate goodness and inexhaustible enthusiasm. The valuable hours of discussion and suggestions that I had with him have undoubtedly helped in supplementing my thoughts in the right direction for attaining the desired objective. I consider myself extremely fortunate for having got the opportunity to learn and work under his able supervision over the entire period of my association with him.

My sincere thanks to all faculty members of Measurement & Instrumentation for their constant encouragement, caring words, constructive criticism and suggestions towards the successful completion of this work.

I do acknowledge with immense gratitude the timely help and support, which I received from my classmates and the Research Scholars in the “Biomedical Instrumentation Laboratory”. I am also thankful to the staff of this Lab for their kind cooperation.

Last but not least, I’m highly indebted to my parents and family members, whose sincere prayers, best wishes, moral support and encouragement have a constant source of assurance, guidance, strength, and inspiration to me.

(VENKATA GIRISH POTNURU)

ABSTRACT

Pulmonary disease is a major cause of ill-health throughout the world. The diagnosis of these common chest diseases is facilitated by pulmonary auscultation using a stethoscope. Auscultation with a stethoscope has many limitations. It is a subjective process that depends on the individual's own hearing, experience and ability to differentiate between different sound patterns. It is not easy to produce quantitative measurements or make a permanent record of an examination in documentary form. Here in this work we developed instrumentation for recording lung sounds, it consists of hardware for acquiring the signal, amplification and filtering. This filtered signal is digitized and recorded.

Respiratory sounds contain significant information on physiology and pathology of the lungs and the airways. The frequency spectrum and the amplitude of sounds, without adventitious sound components (crackles or wheezes), may reflect airway dimension and their pathologic changes (airway obstruction) or pathologic changes in the pulmonary tissue. These crackles sounds are of non stationary in nature so here we implemented Stationary-Non stationary separating filter whose coefficients are solved by LMS (least mean square) algorithm. Wheezes are musical sounds which are sinusoidal in nature are separated by using Discrete Wavelet Transform. Interference of heart sounds in lung sounds are reduced by spectrogram method with help of RLS (recursive least square) filter.

Contents

	Page No.
Candidates Declaration	i
Acknowledgements	ii
Abstract	iii
List of Figures and Tables	vii
CHAPTER 1 INTRODUCTION	1-13
1.1 Anatomy of Respiratory System	1
1.2 Mechanics of Breathing	4
1.3 Breath Sounds	5
1.3.1 Normal Breath Sounds	5
1.3.2 Abnormal Breath Sounds	8
1.3.3 Adventitious Breath Sounds	8
1.4 Literature Review	11
1.5 Organization of Thesis	13
CHAPTER 2 LUNG SOUND MEASUREMENT	14-23
2.1 Auscultation	14
2.2 Instrumentation for Acquisition of Lung Sound	16
2.2.1 Stethoscope	17
2.2.2 Electret Condenser Microphone	17
2.2.3 Amplification and Filtering	19
2.2.4 Data Acquisition Card	20
2.2.5 Acquired Lung Sounds	21
CHAPTER 3 MATHEMATICAL BACKGROUND FOR ANALYSIS OF LUNG SOUNDS	24-34
3.1 Fourier Transform	24
3.1.1 Limitations of FT	25

3.2	Short time Fourier Transform (STFT)	25
3.2.1	Window Function	25
3.2.2	Limitations of STFT	27
3.3	Wavelet Transform	27
3.3.1	Wavelets	28
3.3.2	Continuous Wavelet Transform(CWT)	28
3.3.3	Reconstruction of original time-domain signal from its CWT: Admissibility Condition	29
3.3.4	Multi- Resolutional Approach (MRA)	30
3.3.5	Sampling and the Discrete Wavelet Series	31
3.3.6	Discrete Wavelet Transform (DWT)	32
3.3.7	Reconstruction of original time-domain signal from its DWT	33
CHAPTER 4 LUNG SOUND ANALYSIS		35-67
4.1	Frequency Domain Analysis	36
4.1.1	Analysis with Fourier Transform	36
4.1.2	Analysis with STFT	37
4.1.3	Analysis with Wavelet Transform	39
4.2	Separation of Fine Crackles from Vesicular Sounds By Nonlinear Digital Filter	43
4.2.1	The Stationary-Nonstationary Separating Filter	44
4.2.2	Least Mean Square Algorithm	47
4.2.3	Implementation of basic LMS algorithm	49
4.2.4	Results	49
4.3	Wheeze Episode Detector Using DWT	51
4.3.1	Wheeze Episode Detector	52
4.3.2	Wheeze Identification	52
4.3.3	Wheeze Denoising	54
4.3.4	Results	56

4.4	Heart Sound Reduction in Lung Sounds by Spectrogram	60
4.4.1	Heart Sound Localization by Spectrogram	61
4.4.2	Heart Sound Filtering by RLS-ANC Adaptive Filter	62

CHAPTER 5 CONCLUSIONS AND SCOPE FOR FUTURE

WORK	68-69
REFERENCES	70-72
APPENDIX – I	73-86

List of Figures and Tables

Sl No	Figure No.	Title	Page No.
1	1.1	Anatomy of respiratory system	1
2	1.2	Respiratory tract	2
3	1.3	Alveoli and Capillary Network	3
4	1.4	Physiology of Gas Exchange	4
5	1.5	Normal Vesicular Sounds	6
6	1.6	Bronchial Breath Sounds	7
7	1.7	Bronchovesicular Breath Sounds	7
8	1.8	Fine Crackles	8
9	1.9	Wheezes	9
10	1.10	Stridor	10
11	2.1	Locations on Anterior of Chest	15
12	2.2	Locations on Posterior of Chest	15
13	2.3	Block Diagram Representation of Measurement System	16
14	2.4	Schematic Diagram of an Electret Microphone	17
15	2.5	Microphone Used –Ahuja ATP-20M	18
16	2.6	Sensing Unit	19
17	2.7	Circuit Diagram amplifier and Filter	19
18	2.8	PCL-206	21
19	2.9	Sample1 of Recorded Signals	21
20	2.10	Time Expanded Analysis of Sample1(inspiration)	21
21	2.11	Time Expanded Analysis of Sample1(expiration)	22
22	2.12	Sample2 of Recorded signals	22

23	2.13	Time Expanded Analysis of Sample2(inspiration)	22
24	2.14	Time Expanded Analysis of Sample2(expiration)	23
25	3.1	Example of Window Used for STFT	26
26	3.2	Rectangular Window	26
27	3.3	Time Frequency Resolution at Different Signal Representations	30
28	3.4	Three Level Wavelet Decomposition Tree	33
29	3.5	Three Level Wavelet Reconstruction Tree	34
30	4.1	Raw Signal of Normal Vesicular Sounds	36
31	4.2	Fourier Transform of Normal Vesicular Sounds	36
32	4.3	Raw Signal of Crackles	37
33	4.4	Hanning Window of 256 Samples	38
34	4.5	Spectrogram of Crackles	38
35	4.6	Raw Signal Sampling Frequency (Fs):11025Hz	39
36	4.7	Inspiratory and Expiratory Periods Normal Lung Sounds	40
37	4.8	Raw Lung Sounds With Crackles	40
38	4.9	An Ideal Crackle	41
39	4.10	Identified Crackles in 5 th level Decomposition	41
40	4.11	Raw Signal Lung Sounds With Wheezes	42
41	4.12	Identified Wheezes	42
42	4.13	Schematic Diagram of ST-NST filter	45
43	4.14	Definition of Non-Linear Function	46
44	4.15	The Basic Wiener Filter	47
45	4.16	Raw Crackles With Separation of Crackles	49
46	4.17	Raw Crackles With Separation of Crackles for Sample2	50
47	4.18	Raw Crackles With Separation of Crackles for Sample3	50

48	4.19	Raw Signal of Wheezes	53
49	4.20	Identified Wheezes	53
50	4.21	Simplified Block Diagram of DWT-WED Scheme	54
51	4.22	Separated Wheezes from Breath Sounds	55
52	4.23	Original Signal and Reconstructed signal(without wheezes)	55
53	4.24	Raw Signal with Wheezes	56
54	4.25	Detected Wheezes after Decomposition	56
55	4.26	Separated Wheezes from Breath Sounds	57
56	4.27	Raw Signal and Reconstructed Signal(without wheezes)	57
57	4.28	Raw Signal with Wheezes	58
58	4.29	Detected Wheezes after Decomposition	58
59	4.30	Separated Wheezes from Breath Sounds	59
60	4.31	Raw Signal and Reconstructed Signal(without wheezes)	59
61	4.32	Spectrogram of Lung Sounds with Heart Sounds	61
62	4.33	Reference Signal for Heart Sounds	62
63	4.34	Block Diagram of RLS-ANC filter	63
64	4.35	Spectrogram after Reduction of Heart Sounds	65
65	4.36	Spectrogram of Lung Sounds with Heart Sounds	66
66	4.37	Reference Signal for Heart Sounds	66
67	4.38	Spectrogram after Reduction of Heart Sounds	67

Table No

Title

1	1.1	Breath Sounds	5
2	2.1	Ratings of Components Used	20

CHAPTER-1

INRODUCTION

This chapter discusses about the structure of respiratory system and functions of various organs involved in this system and explain the process how gases are exchanged to supply the oxygen to tissue cells allover the body. Phenomenon of inspiration and expiration are also explained. And explains about different types of breath sounds with waveforms and mentioning the conditions where these occur generally.

1.1. Anatomy of Respiratory System

The exchange of gases in any biological process is termed respiration. The respiratory system is situated in the thorax, and is responsible for gaseous exchange between the circulatory system and the outside world. Air is taken in via the upper airways (the nasal cavity, pharynx and larynx) through the lower airways (trachea, primary bronchi and bronchial tree) and into the small bronchioles and alveoli within the lung tissue. Upper airways and lower airways are as shown in Fig.1.1.

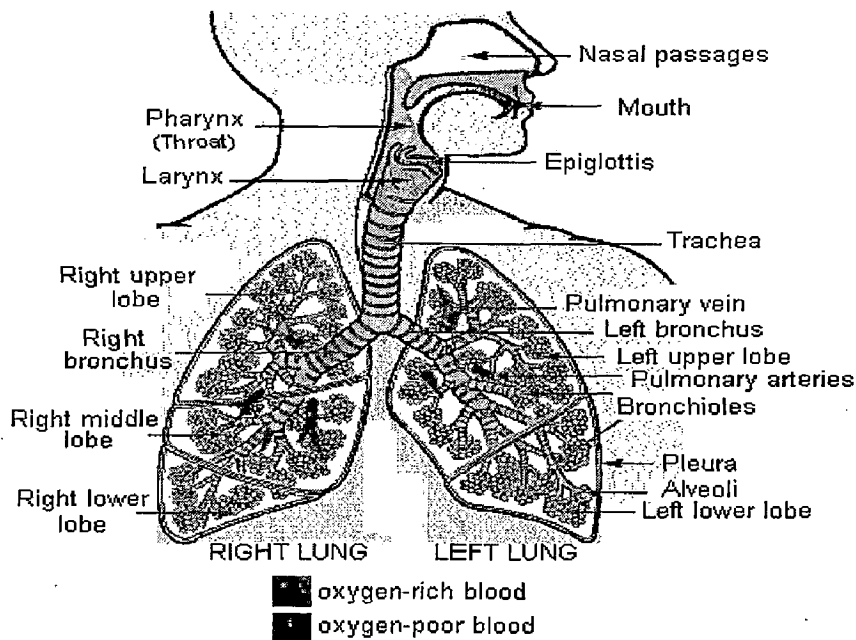


Fig.1.1 Anatomy of respiratory system

The lungs are elastic bags located in closed cavity, called the thorax or thoracic cavity. The right lung consists of three lobes (upper, middle, and lower), and the left lung has two lobes (upper and lower). The larynx, sometimes called the “voice box” (because it contains vocal cords), is connected to the bronchi through the trachea, sometimes called the “windpipe”. Above the larynx is the epiglottis, a valve that closes whenever a person swallows, so that food and liquids are directed to the esophagus (tube leading to the stomach) and into the stomach rather than into the larynx and trachea. The trachea is extending from the larynx to the right and left main stem bronchi.

Functionally the respiratory system structures are separated into conducting zone and respiratory zone.

The *Conducting Zone* consists of the nose, pharynx, larynx, trachea, bronchi, and bronchioles. These structures form a continuous passageway that allows air to move in and out of the lungs. As the air flow through the conducting zone it is also warmed, moistened and cleaned.

The second functional division of respiratory is found deep inside the lungs and is called the *Respiratory Zone*. It is made up of respiratory bronchioles, alveolar ducts, and alveoli. These thin walled structures form a region where gases can be exchanged with nearby capillaries.

Automatically, these same structures are often divided into the *Upper* and *Lower Respiratory Tracts*.

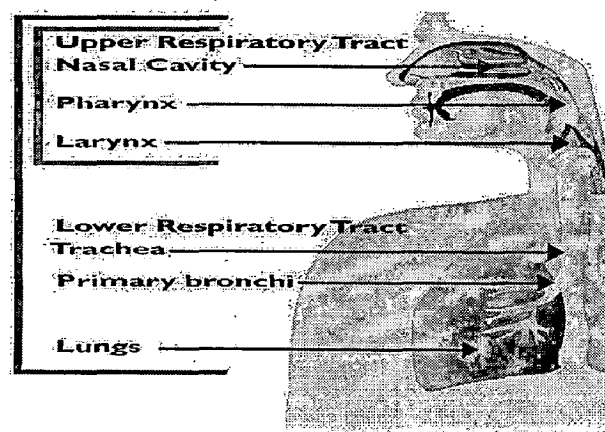


Fig.1.2 Respiratory tract

The *Upper Respiratory Tract* formed by nose, pharynx, and larynx, which are located in the head and neck. *Lower Respiratory Tract* formed by the trachea, bronchi, and lungs (bronchioles, alveoli ducts and alveoli), which are located in thorax (chest).

As the passes through the respiratory tract it came to lower respiratory tract it enters into Bronchus. Each bronchus enters into the corresponding lung and divides like the limbs of a tree into smaller branches. Farther along these branchings, where the diameter is reduced to about 0.1cm, the air-conducting tubes are called bronchioles. As they continue to decrease in size to about 0.05 cm in diameter, they form the terminal bronchioles, which branch again into the respiratory bronchioles, where some alveoli are attached as small air sacs in the walls of the lung. After some additional branching, these air sacs increase in number, becoming the pulmonary alveoli. The alveoli are each about 0.02 cm in diameter. It is estimated that some 300 million alveoli are found in the lungs.

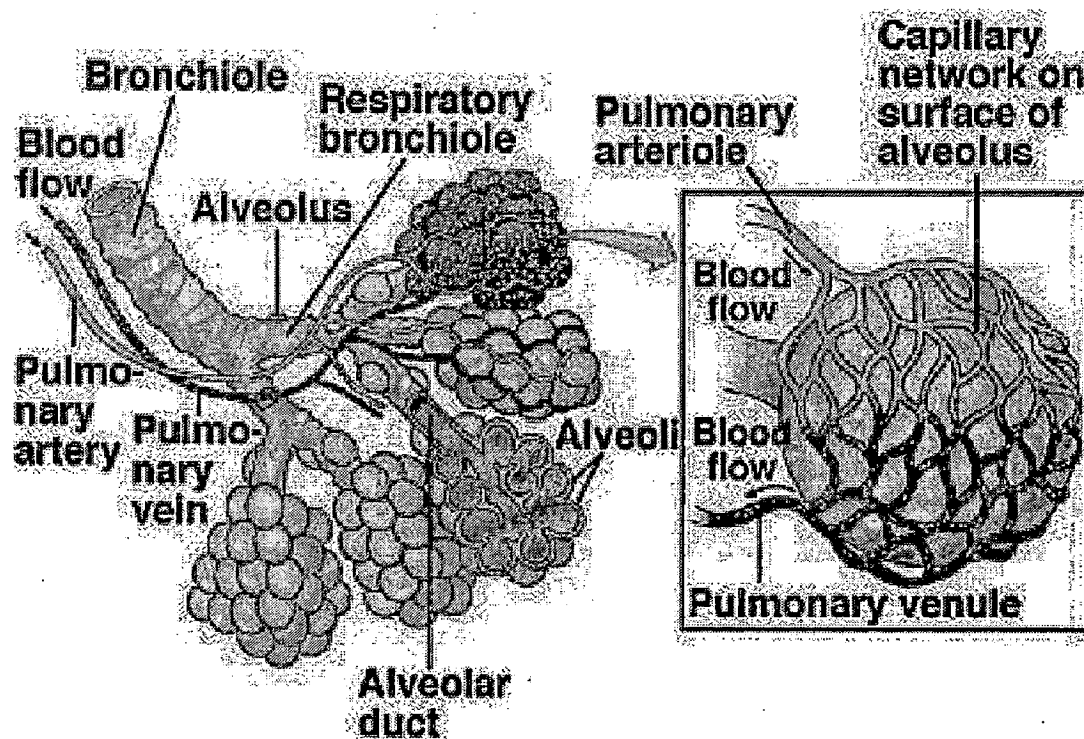


Figure.1.3 Alveoli and capillary network

1.2. Mechanics of Breathing

To take a breath in, the *external intercostal muscles* contract, moving the ribcage up and out. The *diaphragm* moves down at the same time, creating negative pressure within the thorax. The lungs are held to the thoracic wall by the *pleural membranes*, and so expand outwards as well. This creates negative pressure within the lungs, and so air rushes in through the upper and lower airways.

Expiration is mainly due to the natural elasticity of the lungs, which tend to collapse if they are not held against the thoracic wall. This is the mechanism behind lung collapse if there is air in the pleural space (*pneumothorax*).

Each branch of the bronchial tree eventually sub-divides to form very narrow terminal bronchioles, which terminate in the alveoli. There are many millions of alveoli in each lung, and these are the areas responsible for gaseous exchange, presenting a massive surface area for exchange to occur over.

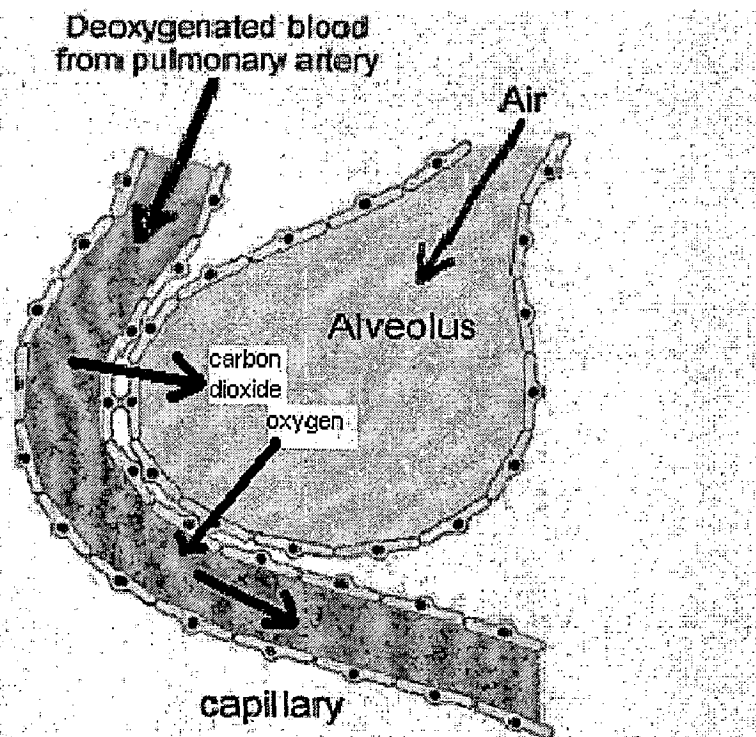


Fig.1.4 Physiology of gas exchange

Each alveolus is very closely associated with a network of capillaries containing deoxygenated blood from the pulmonary artery. The capillary and alveolar walls are very thin, allowing rapid exchange of gases by passive diffusion along concentration gradients.

CO₂ moves *into* the alveolus as the concentration is much lower in the alveolus than in the blood, and O₂ moves *out of* the alveolus as the continuous flow of blood through the capillaries prevents saturation of the blood with O₂ and allows maximal transfer across the membrane.

1.3. Breath Sounds

Breath sounds can be divided and subdivided into the following categories:

Normal	Abnormal	Adventitious
tracheal	absent/decreased	crackles (rales)
vesicular	bronchial	wheeze
bronchial		rhonchi
bronchovesicular		stridor
		pleural rub
		mediastinal crunch

Table.1.1 Breath sounds

1.3.1. Normal Breath Sounds

These are traditionally organized into categories based on their intensity, pitch, location, and inspiratory to expiratory ratio. Breath sounds are created by turbulent air flow. In inspiration, air moves into progressively smaller airways with the alveoli as its final location. As air hits the walls of these airways, turbulence is created and produces sound. In expiration, air is moving in the opposite direction towards progressively larger airways. Less turbulence is created, thus normal expiratory breath sounds are quieter than inspiratory breath sounds.

Tracheal Breath Sound

Tracheal breath sounds are very loud and relatively high-pitched. The inspiratory and expiratory sounds are more or less equal in length. They can be heard over the trachea which is not routinely auscultated.

Vesicular Breath Sound

The vesicular breath sound is the major normal breath sound and is heard over most of the lungs. They sound soft and low-pitched. The inspiratory sounds are longer than the expiratory sounds. Vesicular breath sounds may be harsher and slightly longer if there is rapid deep ventilation (e.g. post-exercise) or in children who have thinner chest walls. As well, vesicular breath sounds may be softer if the patient is frail, elderly, obese, or very muscular.

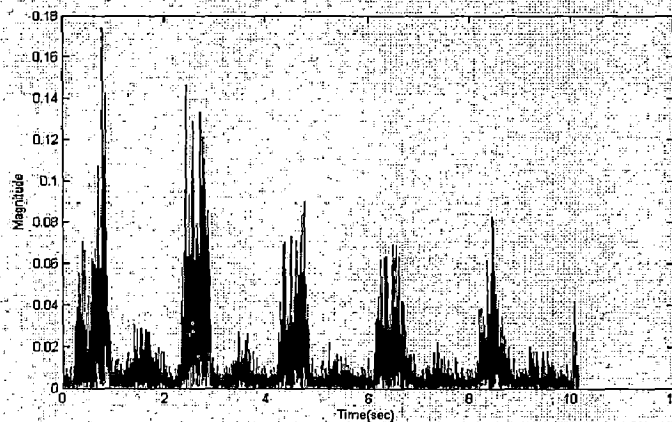


Fig.1.5 Normal vesicular sounds

Bronchial Breath Sound

Bronchial breath sounds are very loud, high-pitched and sound close to the stethoscope. There is a gap between the inspiratory and expiratory phases of respiration, and the expiratory sounds are longer than the inspiratory sounds. If these sounds are heard anywhere other than over the manubrium, it is usually an indication that an area of consolidation exists (i.e. space that usually contains air now contains fluid or solid lung tissue).

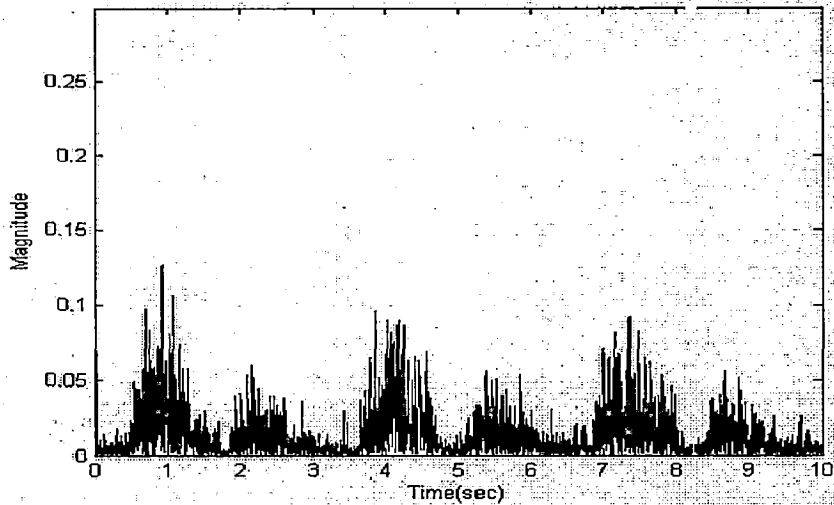


Fig.1.6 Bronchial breath sound

Bronchovesicular Breath Sound

These are breath sounds of intermediate intensity and pitch. The inspiratory and expiratory sounds are equal in length. They are best heard in the 1st and 2nd ICS (anterior chest) and between the scapulae (posterior chest) - i.e. over the mainstem bronchi. As with bronchial sounds, when these are heard anywhere other than over the mainstem bronchi, they usually indicate an area of consolidation.

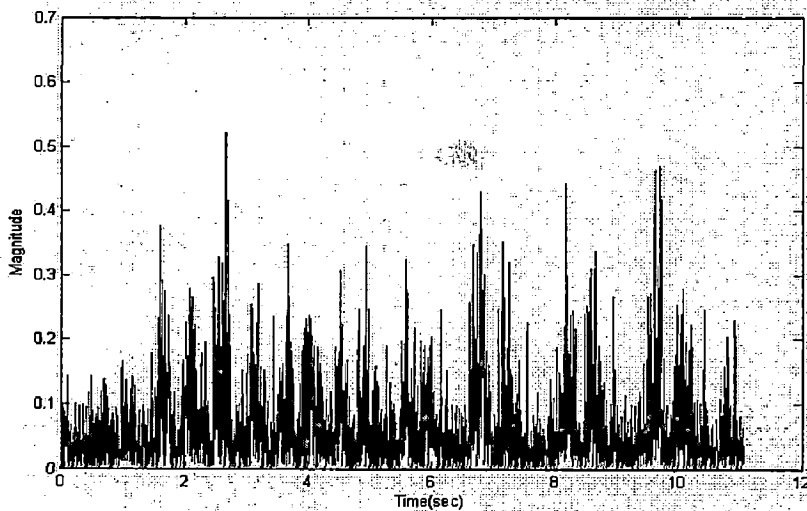


Fig.1.7 Bronchovesicular breath sounds

1.3.2. Abnormal Breath Sounds

Absent or Decreased Breath Sounds

There are a number of common causes for abnormal breath sounds, including:

- *Asthma*: decreased breath sounds
- *Atelectasis*: If the bronchial obstruction persists, breath sounds are absent unless the atelectasis occurs in the RUL in which case adjacent tracheal sounds may be audible.
- *Emphysema*: decreased breath sounds
- *Pleural Effusion*: decreased or absent breath sounds. If the effusion is large, bronchial sounds may be heard.
- *Pneumothorax*: decreased or absent breath sounds

Bronchial Breath Sounds in Abnormal Locations

Bronchial breath sounds occur over consolidated areas. Tests like egophony and whispered petroliloquy may confirm the suspicions.

1.3.3. Adventitious Breath Sounds

Crackles (Rales)

Crackles are discontinuous, nonmusical, brief sounds heard more commonly on inspiration. They can be classified as fine (high pitched, soft, very brief) or coarse (low pitched, louder, less brief). Crackles may sometimes be normally heard at the anterior lung bases after a maximal expiration or after prolonged recumbency.

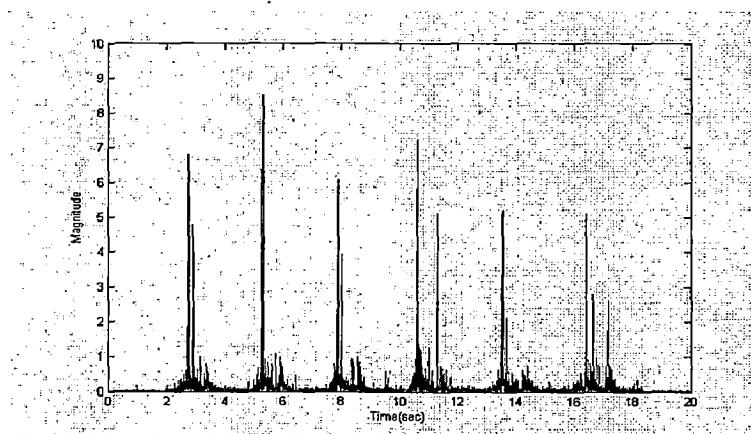


Fig.1.8 Fine crackles

The mechanical basis of crackles: Small airways open during inspiration and collapse during expiration causing the crackling sounds. Another explanation for crackles is that air bubbles through secretions or incompletely closed airways during expiration.

Conditions: asthma, bronchiectasis, chronic bronchitis, consolidation, interstitial lung disease, pulmonary edema

Wheezes

Wheezes are continuous, high pitched, hissing sounds heard normally on expiration but also sometimes on inspiration. They are produced when air flows through airways narrowed by secretions, foreign bodies, or obstructive lesions. When the wheezes occur and there is a change after a deep breath or cough.

Conditions: asthma, chronic bronchitis, pulmonary edema.

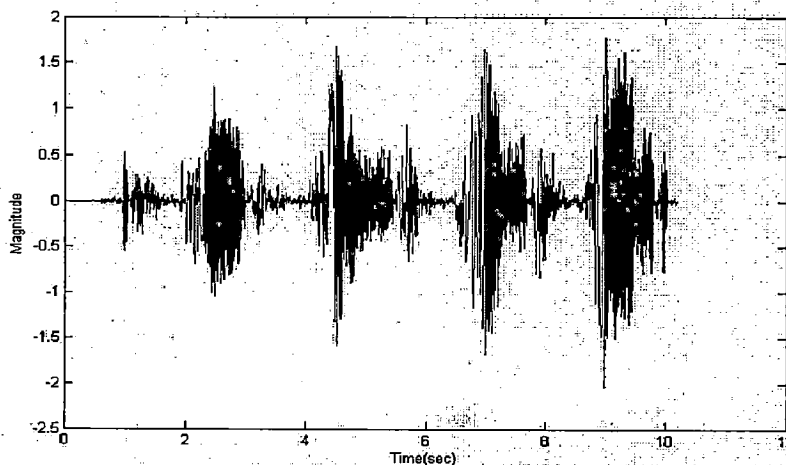


Fig.1.9 Wheezes

Rhonchi

Rhonchi are low pitched, continuous, musical sounds that are similar to wheezes. They usually imply obstruction of a larger airway by secretions.

Stridor

Stridor is an inspiratory musical wheeze heard loudest over the trachea during inspiration. Stridor suggests an obstructed trachea or larynx and therefore constitutes a medical emergency that requires immediate attention.

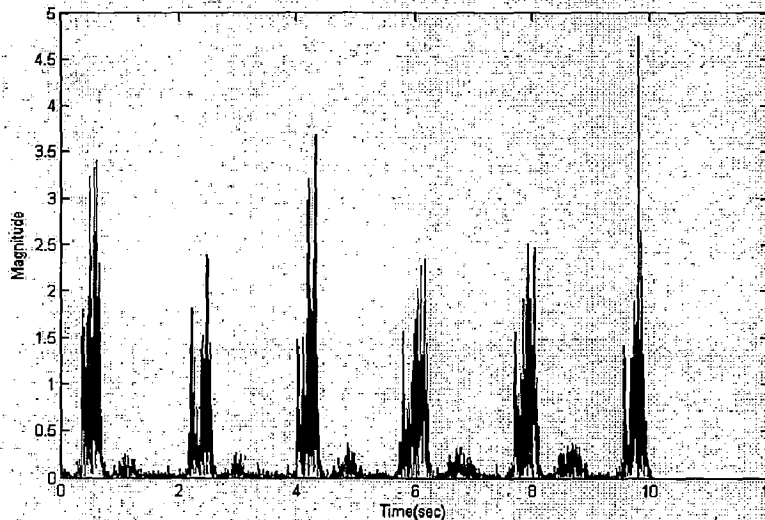


Fig.1.10 Stridor

Pleural Rub

Pleural rubs are creaking or brushing sounds produced when the pleural surfaces are inflamed or roughened and rub against each other. They may be discontinuous or continuous sounds. They can usually be localized a particular place on the chest wall and are heard during both the inspiratory and expiratory phases.

Conditions: pleural effusion, pneumothorax.

Mediastinal Crunch

Mediastinal crunches are crackles that are synchronized with the heart beat and not respiration. They are heard best with the patient in the left lateral decubitus position. As with stridor, mediastinal crunches should be treated as medical emergencies.

Conditions: pneumomediastinum.

1.4. Literature Review

Developing a harddisk recording system with high sampling rates of three channels to examine the possibility for a sound pattern detection system and applied it in patients and healthy volunteers was proposed in [1]. Kahya.Y.P etc in[2] and [3] proposed multi channel recording with DSP processor and processed those signals in real time and classification is also done.

B. Widrow, I. M. McCool, in [4] described the performance characteristics of the LMS adaptive filter, a digital filter composed of a tapped delay line and adjustable weights, whose impulse response is controlled by an adaptive algorithm. Benedetto.G, Dalmaso.F,[7] explains the characteristic of crackles and diagnostic importance.

The timing, repeatability, and shape of crackles are important parameters for diagnosis. Therefore, automatic detection of crackles and their classification as fine and coarse crackles have important clinical value. Since the multiresolution decomposition technique can give high resolution in both time and frequency, it can be exploited to detect crackles and classify them according to the information in each scales. F.K. Lam, F.H.Y. Chan [8] present new methods for crackle detection based on continuous wavelet transform. In [9], proposed a new method for crackle detection which is based on 'matched' wavelet transform.

In order to separate the crackles from vesicular sounds automatically, Mariko.O, Kaoru Arakawa[10] proposed a nonlinear digital filter which was designed to separate nonstationary from stationary signals, and this filter coefficients were derived by LMS algorithm.

An algorithm has been designed to achieve a high sensitivity to wheezing sound detection [11] and [12]. Wheezes detection was also desired to be independent from respiratory sound power.

The identification of continuous abnormal lung sounds, like wheezes, in the total breathing cycle is of great importance in the diagnosis of obstructive airways pathologies. To this vein, the Taplidou.S.A, Hadjileontiadis.L.J, [13] introduced an efficient method for the detection of wheezes, based on the time-scale representation of breath sound recordings. The employed Continuous Wavelet Transform is proven to be a valuable tool at this direction, when combined with scale-dependent thresholding. Analysis of lung sound recordings from wheezing patients shows promising performance in the detection and extraction of wheezes from the background noise and reveals its potentiality for data-volume reduction in long-term wheezing screening, such as in sleep-laboratories.

Depending on pulmonary airflow, sensor location, and individual physiology, heart sounds may obscure lung sounds in both time and frequency domains, and thus pose a challenge for development of semi-automated diagnostic techniques. Gnitecki.J, Moussavi.Z,[15] proposed a recursive least squares (RLS) adaptive noise cancellation (ANC) filtering which had applied for heart sounds reduction in lung sounds. This algorithm in [16] uses an image processing technique to detect HN segments in the spectrogram of the recorded lung sound signal. Afterwards the algorithm removes those segments and estimates the missing data employing a 2D interpolation in the time-frequency domain and finally reconstructs the signal in the time domain.

Adaptive Filtering is an accepted method to intelligently remove the heart sound from the lung sounds. However the drawback of the adaptive noise canceling scheme is the need of a reference signal that is exactly in the same time alignment as the interference signal in the primary signal. E. Saatci, A.Akan proposed in[16] a effective and easy method based on Spectrogram is presented to automatically generate a reference signal from the lung sound signal. Adaptive Noise Cancelation with Recursive Least Square (RLS-ANC) method is used to filter out the heart sound from lung sound.

1.5. Organization of Thesis

This Thesis is organized in the following way:

In Chapter-2, I have explained the Hardware Setup used for the acquisition of Lung sounds with help of block diagram. Each component of setup was explained with its specifications and recorded wave forms of lung sounds are also shown.

Chapter-3 explains various signal processing techniques with their limitations. These techniques are going to be used in the analysis of lung sounds.

Chapter-4 presents various adaptive filter techniques and other processing techniques to remove the adventitious sounds like crackles and wheezes. Another technique was presented to reduce the interference of heart sounds in lung sounds. Every method was explained with help of results.

Chapter-5, conclusions and scope for future work are given.

CHAPTER-2

LUNG SOUND MEASUREMENT

Measurement of lung sounds widely used in the analysis of pulmonary diseases. Stethoscope is widely used for this purpose but as per diagnostic requirements due to so many reasons it is not suitable. This chapter discusses about development of equipment and explains various components used in this equipment.

2.1. Auscultation

Auscultation is one of the widely used techniques for listening Breath Sounds. These sounds can be heard either on the chest or at the posterior of the chest. These are the certain precautions that should be followed for auscultation:

- a) It is important to create a *quiet environment* as much as possible. Eliminate noise by closing the door and turning off any radios or televisions in the room.
- b) The patient should be in the *proper position* for auscultation, i.e. sitting up in bed or on the examining table, ensuring that his or her chest is not leaning against anything.
- c) Stethoscope should be touching the patient's *bare skin* whenever possible or we may hear rubbing of the patient's clothes against the stethoscope and misinterpret them as abnormal sounds. We can wet the patient's chest hair with a little warm water to decrease the sounds caused by friction of hair against the stethoscope.
- d) Be considerate and warm the diaphragm of our stethoscope with our hand before auscultation.

It is important that we always compare what we hear with the opposite side. Example if we are listening to the left apex, we should follow through by comparing what we heard with what we hear at the right apex.

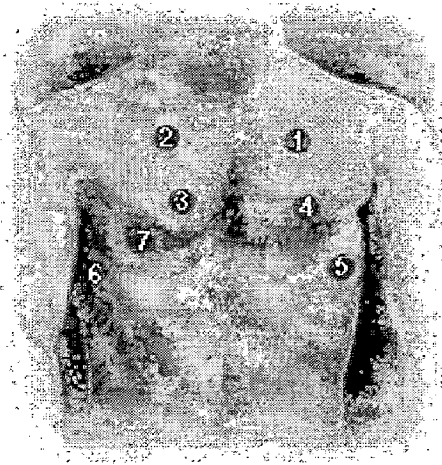


Fig.2.1 Locations on anterior of chest

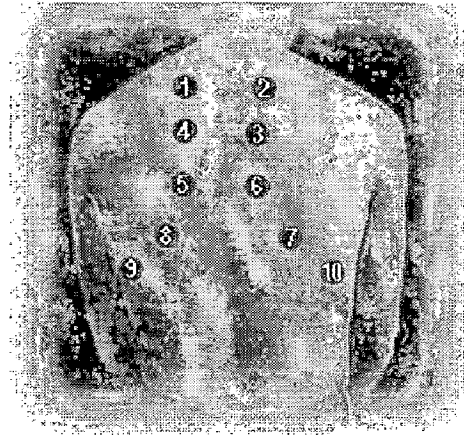


Fig.2.2 Locations on posterior of Chest

There are 12 and 14 locations for auscultation on the anterior and posterior chest respectively. Generally, we should listen to at least 6 locations on both the anterior and posterior chest. Begin by auscultating the apices of the lungs, moving from side to side and comparing as we approach the bases. Making the order of the numbers in the Fig.2.1 and Fig.2.2 a ritual part of our pulmonary exam is a way of ensuring that we compare both sides every time and we'll begin to know what each area should sound like under normal circumstances. If we hear a suspicious breath sound, listen to a few other nearby locations and try to delineate its extent and character.

However, traditional auscultation with a stethoscope does not meet the requirements for a diagnostic test due to, primarily, limitations of human ear auditory system.

- The ears are sensitive to deterministic sounds in the time or frequency domains, but are substantially less accurate in identifying, analyzing, and classifying the noise.
- Another reason for human deficiency in the analysis of lung sounds is their low signal-to-noise ratio. Thoracic lung sounds have relatively low amplitude compared with background noise of heart and muscle sounds. Because of the lack of objectivity, and the qualitative nature of lung sounds, many physicians no longer rely on auscultation as a diagnostic tool.

The application of computer technology has provided new insights into acoustic mechanisms and new measurements of clinical relevance on lung sounds. The use of digital signal processing techniques to extract information on average sounds were major steps that have advanced the utility of lung sounds beyond the stethoscope. The breathing associated sound heard on the chest of a healthy person is called the normal lung sound. The normal lung sound is characterized by larger, louder sounds during inspiration than during expiration.

Although lung sounds provide important information about the respiratory system, the analysis of lung sounds has not been widely used in clinical practice because of the complicated procedure involved. However, computer technology has made impressive advancements in recent years. Today, practically all personal computer models are equipped with the capacity for audio-signal input and output. In this study, we developed a computer-based system for lung sounds acquisition.

2.2. Instrumentation for Acquisition of Lung Sound

A block diagram representation of the measurement system is shown as under [1].

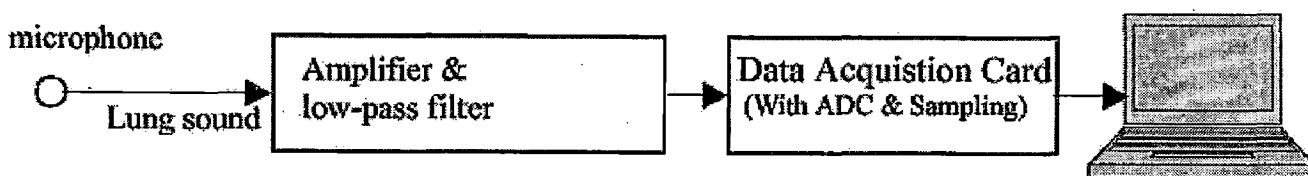


Fig.2.3 Block diagram representation of measurement system

Equipments Used and Their Specifications:

1. Stethoscope
2. Electret Condenser Microphone
3. Electronic Components. (OP-AMPs, Resistors, Capacitors)
4. Data Acquisition Card (PCL-206)

2.2.1. Stethoscope

Stethoscopes are not only useful for doctors, but home mechanics, exterminators, spying and many numbers of other uses. A standard stethoscope meant for clinical interest is used to detect the lung's sound signals of a human body. Standard stethoscopes provide no amplification which limits their use. Amplification of the signals is needed so that they can be used according to the desired purpose, which can be done by an amplifier of suitable gain. The sound signals detected by stethoscope can be converted into analog form using an electret's microphone. The head of the stethoscope is cut off and a small piece of rubber tube is used to join the nipple on the head to the microphone.

2.2.2. Electret Condenser Microphone

Introduction

Electret's Condenser Microphones (ECM) are used in almost every consumer and communication audio application. The most commonly used ECM's consist of a JFET inside an electret microphone canister, which acts as a buffer between the capacitive sensor and the output. JFET's are small, three-terminal devices that have been improved toward very small, low cost plastic packages. This enabled the main innovation of ECM, their increasingly smaller sizes. ECM's as small as 2mm in height are common. With a stack of condenser microphone plates and spacers, this requires packaged JFET's as small as 0.5mm in thickness. A cross sectional view of a typical ECM is shown in Fig 2.5.

(Refer Appendix 1 for specifications of Microphone).

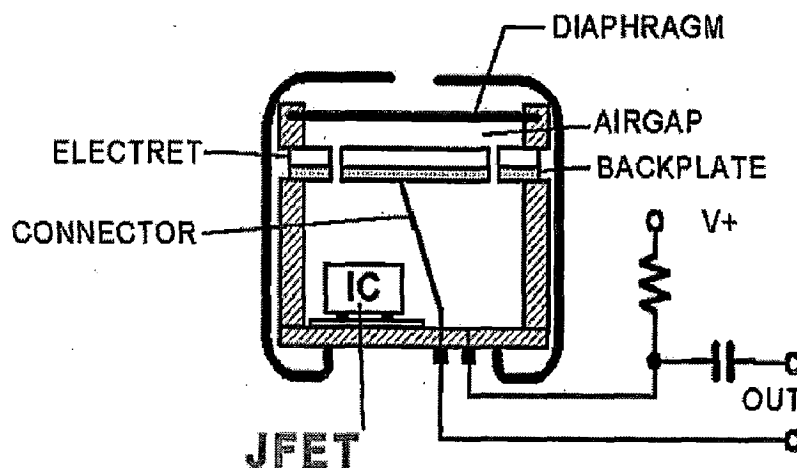


Fig.2.4 Schematic diagram of an electret microphone

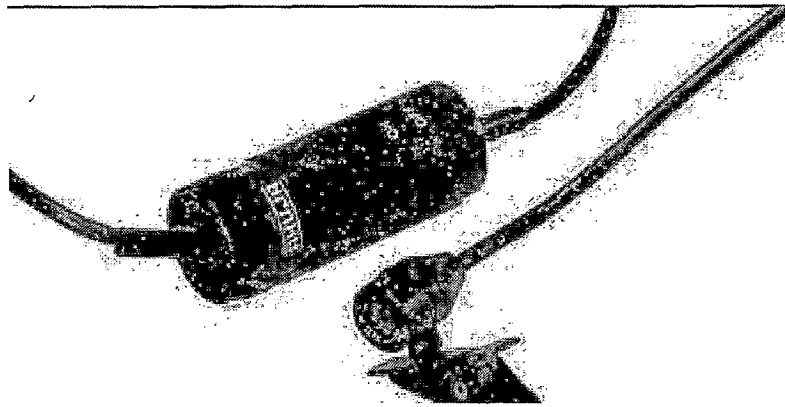


Fig.2.5 Microphone Used- Abuja ATP-20M

Biasing and Interfacing the ECM

An Electret's microphone consists of a pre-charged, non-conductive membrane between 2 plates that form a capacitor. One of the plates is fixed and the other plate moves with sound pressure. Movement of the plate results in a capacitance change, which in turn results in a change in output voltage due to the non-conductive, pre-charged membrane. An electrical representation of such an acoustic sensor consists of a signal voltage source in series with a source capacitor. The most common method of interfacing this sensor has been a high impedance buffer/amplifier. A single JFET with its gate connected to the sensor plate and biased as shown in Fig. provides the following properties:

- Signal buffering
- High pass filtering
- Self-biasing of active components
- External phantom biasing

The main benefits of this type of ECM are its small size, low cost and relatively low noise. However, the combination of a single JFET and low load resistor results in a low gain (typically -3 dB) and therefore low sensitivity of the ECM. A low sensitivity of the ECM results in small output voltages of the sensor (on the order of 0.1-10mV average, 100mV peak). To make such a microphone work in a system (such as a mobile phone) requires careful board design, along with additional filtering components, to keep a

reasonable signal-to-interference ratio. Also, to supply the signal to an Analog-to-Digital (ADC) converter, significant pre-amplification is necessary. The microphone (Abuja ATP-20M) was attached to stethoscope chest piece (Microtone) via 5-cm-long rubber tubing. Signals from the microphone-stethoscope chest piece amplified by an OP-AMP and filtered by a Second Order Low Pass Butterworth Filter.



Fig.2.6 Sensing unit.

2.2.3. Amplification and Filtering

The output obtained by the microphone is amplified and filtered by using the following circuit.

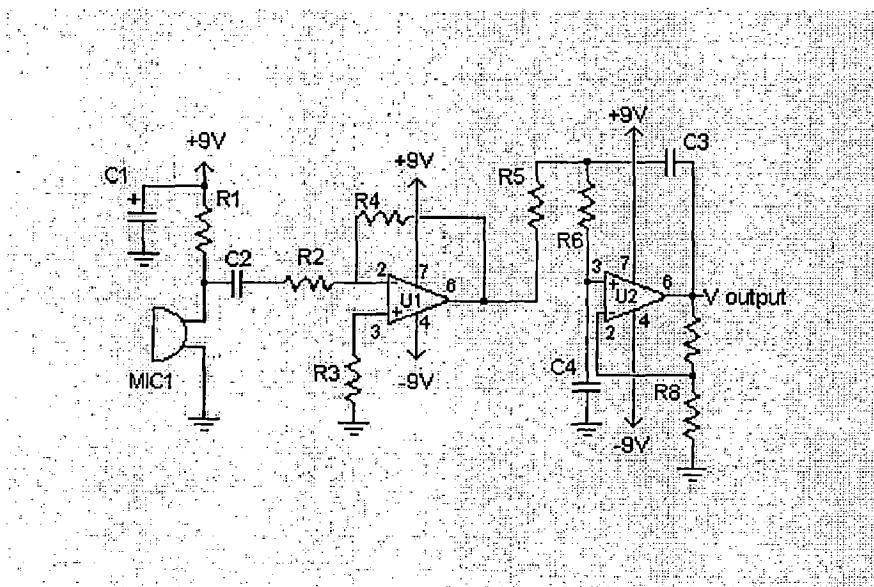


Fig.2.7 Circuit Diagram of amplifier and filter

Electronic Components Used

- 741 op-amps (two).
- Resistors ---- 10K(four), 2.2K(two), 47K(one), 33K(three)
- Capacitors----- 470 μ f(one), 0.047 μ f(three), 0.01 μ f(one)

Table.2.1 Ratings of different components used

R1	1	10K 1/4W Resistor
R2, R3	2	2.2K 1/4W Resistor
R4	1	47K 1/4W Resistor
R5, R6, R7	3	33K 1/4W Resistor
R8	1	56K 1/4W Resistor
C1	1	470uF Electrolytic Capacitor
C2, C3, C4	3	0.047uF Capacitor
U1, U2	2	741 Op-Amp
MIC1	1	Electret Mic
MISC	1	Board, Wire, Sockets for ICs, Stethoscope, Rubber tube

The output of the microphone is given to amplifier whose gain is 21.4. The signals are then send to a second order low pass filter having higher cutoff frequency 102 Hz below which all the important frequency components of respiratory sounds exist. The output of the filter was given to the Data Acquisition Card (PCL-206).

2.2.4. Data Acquisition Card

New developing fields like image processing, transient analysis and biomedical observations started demanding fast A/D and D/A conversions. As IBM-PC is being used for such applications, high speed multifunction A/D and D/A cards became much sought after commodities. Such Add-On cards with fast, high precision A/D converter turns IBM-PC into data acquisition and signal analysis instrument. PCL-206 is an IBM-PC/XT/AT compatible multifunction analog input card, which has many desirable advanced features for sophisticated measurements. Specifications of PCL-206 ADC are clearly explained in Appendix-1.

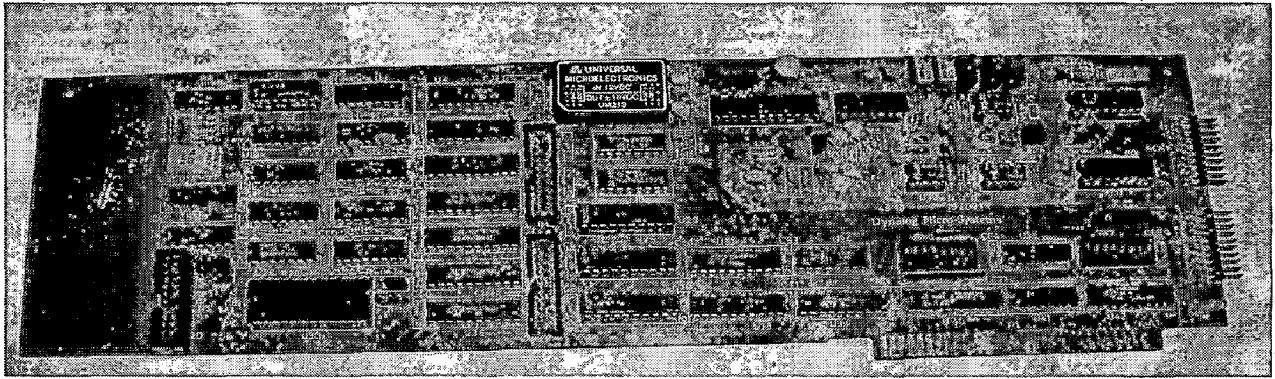


Fig.2.8 PCL-206

2.2.5. Acquired Lung Sounds

A software program was written in Turbo C++ compiler to interface the card. The program gave necessary command words to the hardware ports of PCL-206 and obtained the digital values from the card. The samples taken from two different subjects are shown as under:

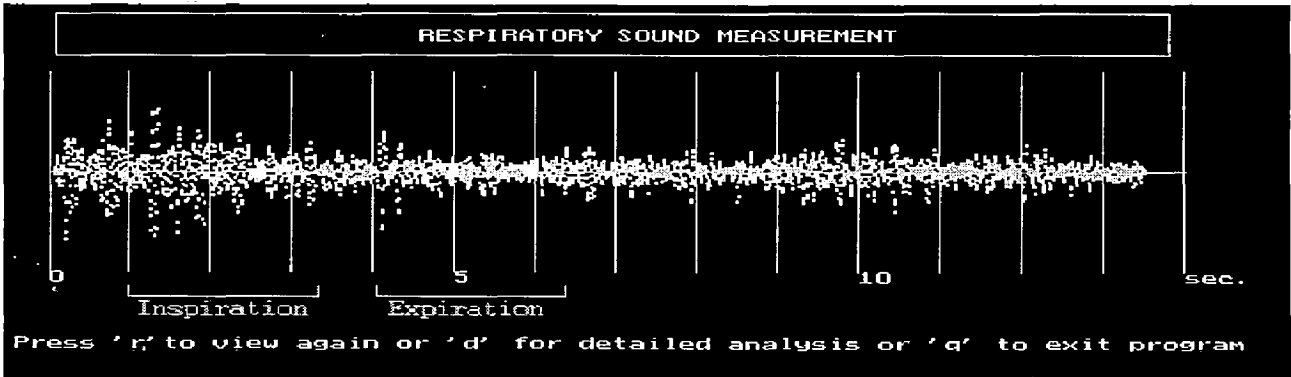


Fig.2.9 Sample 1 of recorded signals

From the above sample we can infer that the magnitude during inspiration is higher than that during expiration

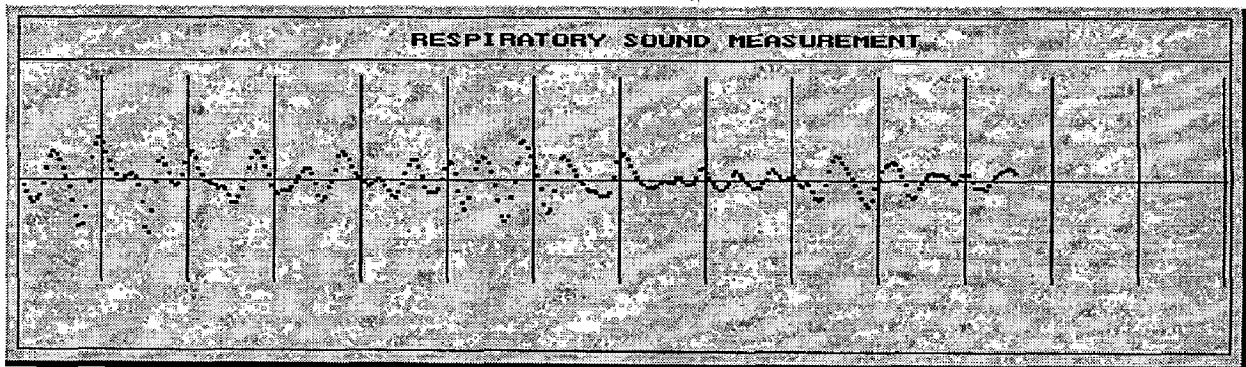


Fig.2.10 Time expanded analysis of sample 1 (inspiration)

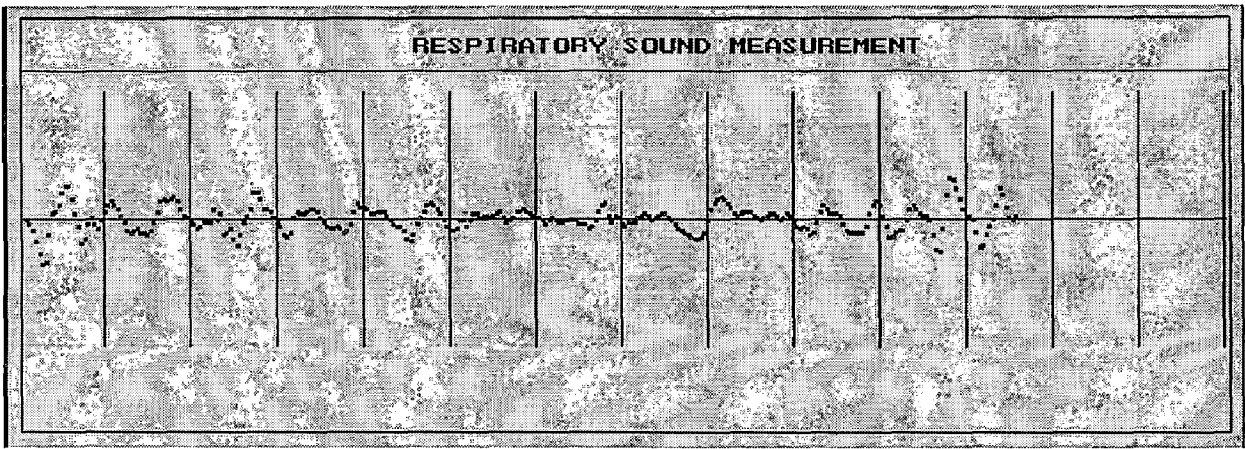


Fig.2.11 Time expanded analysis of sample 1 (expiration)

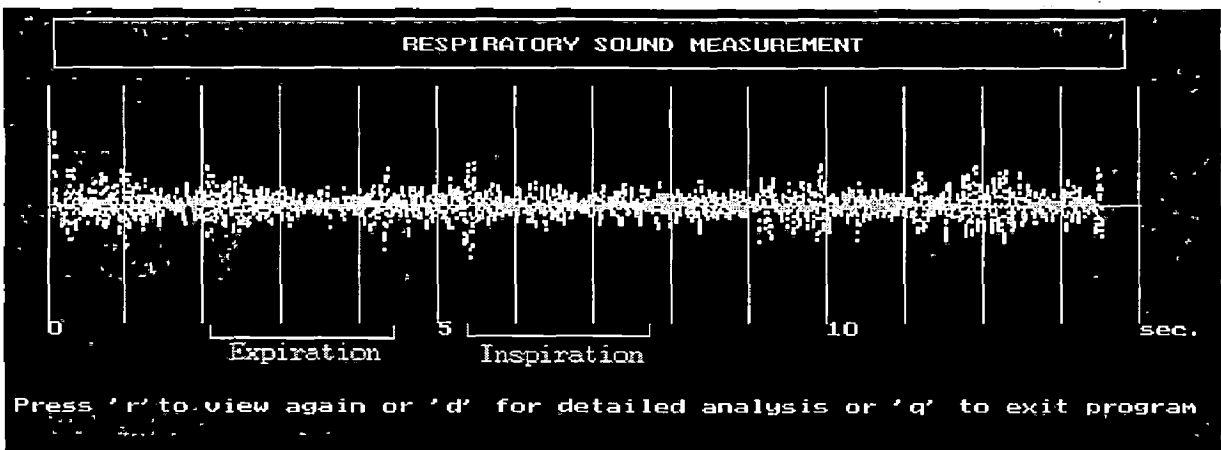


Fig.2.12 Sample 2 of recorded signals

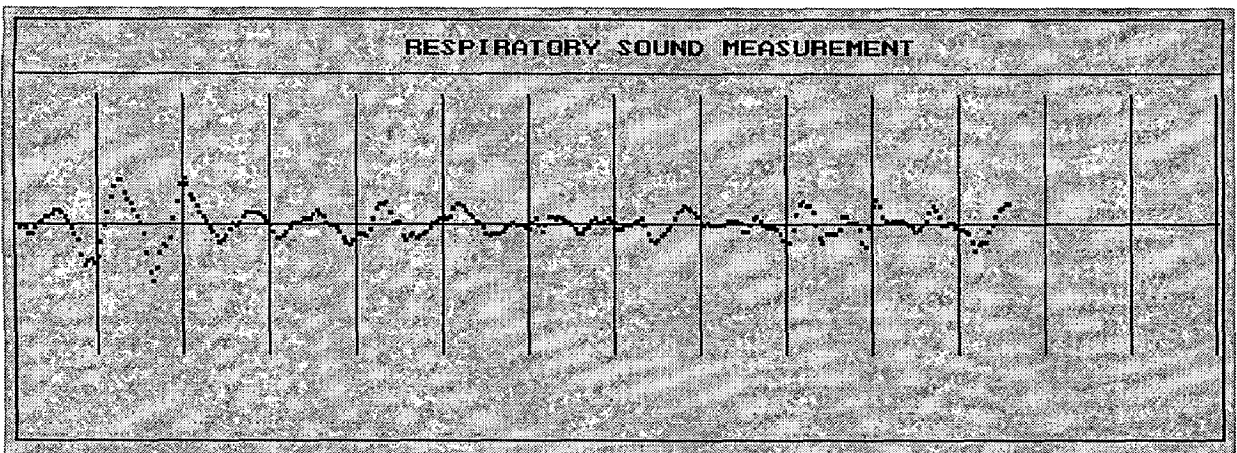


Fig.2.13 Time expanded analysis of sample 2 (inspiration)

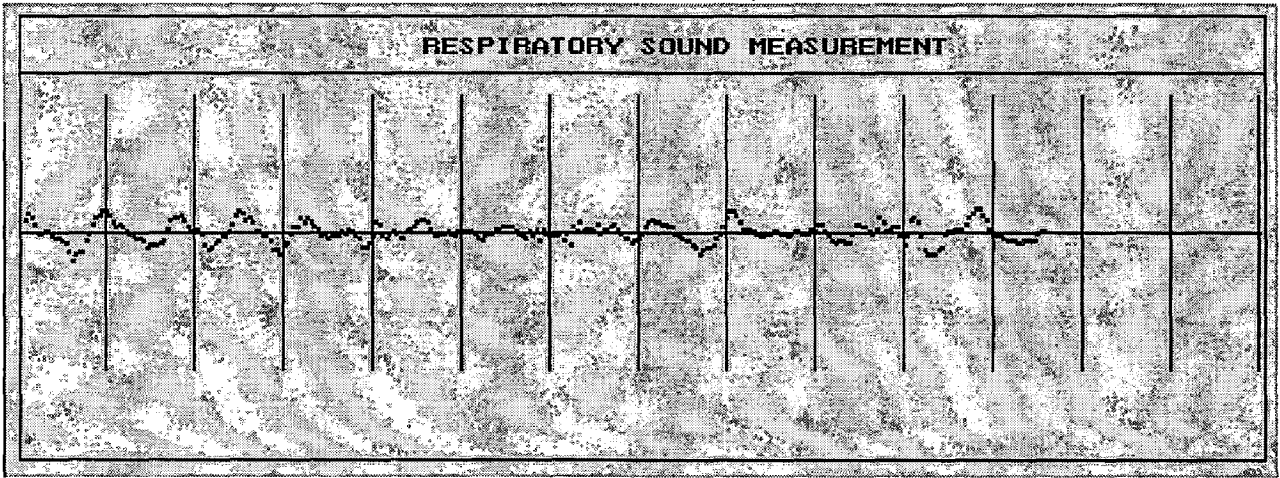


Fig.2.14 Time expanded analysis of sample 2 (expiration)

CHAPTER-3

MATHEMATICAL BACKGROUND FOR ANALYSIS OF LUNG SOUNDS

This chapter discusses various signal processing techniques which are used for analysis of lung sounds. Initially frequency analysis techniques are discussed and after discussing limitations of these methods it will discuss various time frequency analysis techniques.

3.1. Fourier Transform

The Fourier Transform finds itself ubiquitously prevalent in many applications involving the analysis of the frequency content of the signal. Its evolution can be dated back to the 19th century when a French Mathematician J. Fourier showed that any periodic function could be expressed as an infinite sum of periodic complex exponential functions. This was later generalized to both periodic and non-periodic signals and was known as Fourier Transform.

Fourier transforms can be used to translate time domain signals into the frequency domain. It acts as a mathematical prism, breaking up the time signal into frequencies, as a prism breaks light into different colors. Fourier transform decomposes a signal into complex exponential functions of different frequencies. Thus, it gives a complete picture of the frequency components of the signal under consideration.

The following equations can be used to calculate the Fourier transform of a time-domain signal and the inverse Fourier Transform:

$$X(f) = \int_{-\infty}^{\infty} x(t) \cdot e^{-2j\pi ft} dt \quad (3.1)$$

$$x(t) = \int_{-\infty}^{\infty} X(f) \cdot e^{2j\pi ft} df \quad (3.2)$$

Where, x is the original signal, t is time, f is frequency, X is the Fourier transform.

3.1.1. Limitations of FT

Fourier transforms are very useful at providing frequency information that cannot be seen easily in the time domain. However they do not suit brief signals, signals that change suddenly or in fact any non-stationary signals. The reason is that they show only what frequencies occur, not when these frequencies occur, so they are not much help when both time and frequency information is required simultaneously. In stationary signals, all frequency components occur at all times.

3.2. Short time Fourier Transform (STFT)

As explained in section 3.1, the Fourier transform can be used for stationary signals. Hence, in order to analyze the non-stationary signals, small portions of these signals are considered, where they behave as essentially stationary. The same Fourier transform concept is applied to these segmented portions, to analyze the signal in both time and frequency domains simultaneously. Therefore through this technique analysis of frequency components and the positions of occurrence of these frequency components can be accomplished. This analysis can be done using windowing techniques.

3.2.1. Window Function

The STFT looks at a signal through a small window, using the idea that a sufficiently small section of the wave will be approximately a stationary wave and so Fourier analysis can be used. The window is moved over the entire wave, providing some information about what frequencies appear at what time.

A desired portion of a signal can be removed from the main signal by multiplying the original signal by another function, which is zero outside the interval desired. Such a function which helps in extracting the desired portion is called windowing function.

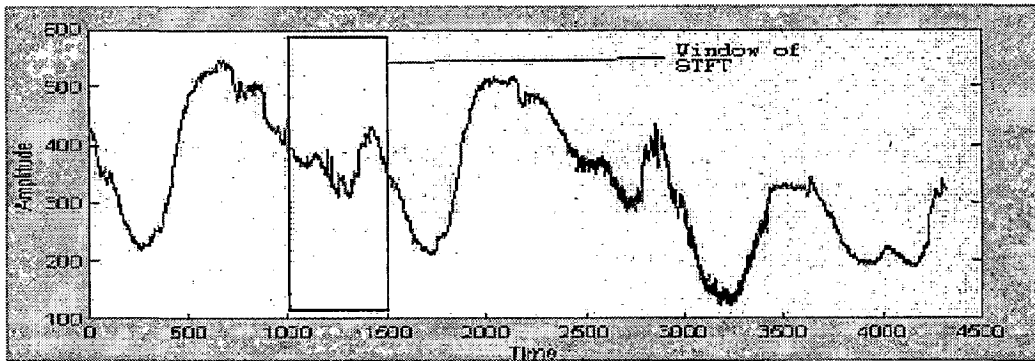


Fig.3.1 Example of a window used for STFT

The following equation can be used to compute a STFT. It is different to the FT as it is computed for particular windows in time individually, rather than computing overall time (which can be alternatively thought of as an infinitely large window). x is the signal, and w is the window.

$$STFT_x^{(w)}(t, f) = \int [x(t) \cdot w^*(t-t')] \cdot e^{-j2\pi ft} dt \quad (3.3)$$

Some of the common window functions are rectangular window, gabber window, Kiser window, cosine window etc. the configuration of rectangular window is specified in equation

$$W_b(t) = W(t) \quad t \in [b-t', b+t']$$

$$= 0 \text{ otherwise} \quad (3.4)$$

These windows are pictorially represented in figure

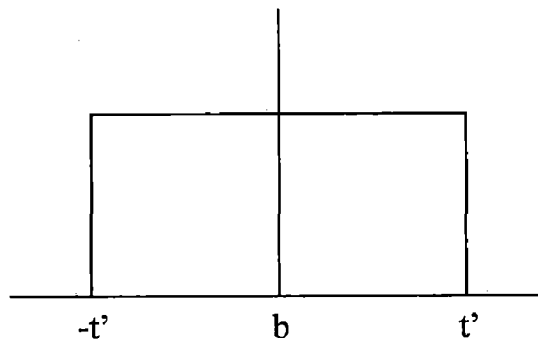


Fig.3.2 Rectangular window

By changing the parameter b , the window function can be sliced to analyze the local behavior of the analyzing signal. Also, the window width can be varied by changing t' .

3.2.2. Limitations of STFT

There is an improvement, as a time domain signal can be mapped onto a function of time and frequency, providing some information about what frequencies occurs when. However using windows, introduces a new problem; it is impossible to know exactly what frequencies occur at what time, only a range of frequencies can be found. This means that trying to gain more detailed frequency information causes the time information to become less specific and visa versa. Therefore when using the STFT, there has to be a sacrifice of either time or frequency information. Having a big window gives good frequency resolution but poor time resolution; small windows provide better time information, but poorer frequency information.

3.3. Wavelet Transform

The beginning of the wavelet transform as a specialized field can be traced to the work of Grossman and Morlet. Their motivation in studying wavelet transforms was provided by the fact that certain seismic signals can be modeled suitably by combining translations and dilations of simple oscillatory function of finite duration known as wavelet.

Wavelet transform is inheritable linear transformation technique, capable of providing the time and frequency information simultaneously, hence giving a time frequency representation of the signal. The wavelet transform was developed as an alternative to the short time Fourier transform to overcome the resolution problem. Wavelet analysis is next logical step to a windowing technique with variable-sized regions. Wavelet analysis allows the use of long time intervals where more precise low frequency information is required and shorter regions where high frequency information is required.

3.3.1. Wavelets

The signals such as seismic signal can be modeled suitably by combining translations and dilations of a simple, oscillatory function of finite duration called a wavelet.

A function $P(t)$ is a mother wavelet, if it satisfies the following two properties.

1. The function integrates to zero:

$$\int P(t)dt = 0$$

2. The signal has finite energy:

$$\int P^2(t)dt \text{ is finite.}$$

There are many types of wavelets used for to compute the wavelet transform of a signal. Different applications dictate the choice of wavelet for the particular application. Some of the most common of these are cubic B-Spline wavelet, Morlet wavelet, Haar wavelet etc.

3.3.2. Continuous wavelet transform (CWT)

In continuous wavelet transform, analysis is done similar to the short time Fourier transform. The signal is multiplied with a function similar to the window function in STFT and transform is computed separately for different segment of time domain signals.

The basic differences between continuous wavelet transform and short time Fourier transform are listed below.

- The Fourier transform of window signals are not taken, therefore signal peak will be seen corresponding to a sinusoid i.e., negative frequencies are not computed.
- The width of the windows is changed as the transform is computed for every single spectral component, which is probably the most significant characteristic of wavelet transform.

The continuous wavelet transform is the sum over all time of scaled and shifted versions of the mother wavelet ψ . Calculating the CWT results in many coefficients C , which are functions of scale and translation.

$$CWT_x^\psi(\tau, s) = \int x(t) \psi_{\tau, s}^* dt \quad (3.5)$$

The basis wavelet functions are derived from a single prototype *Mother Wavelet* as follows

$$\psi_{\tau, s} = \frac{1}{\sqrt{s}} \psi \left(\frac{t - \tau}{s} \right) \quad (3.6)$$

The translation τ is proportional to time information and the scale s is proportional to the inverse of the frequency information. To find the constituent wavelets of the signal, the coefficients should be multiplied by the relevant version of the mother wavelet.

The scale of a wavelet simply means how stretched it is along the x-axis, larger scales are more stretched. The term ' $\frac{1}{\sqrt{s}}$ ' in equation (3.6) serves the purpose of *energy normalization* of the wavelet across various scales.

3.3.3. Reconstruction of original time-domain signal from its CWT: Admissibility Condition

The continuous wavelet transform is a reversible transform, provided that the *admissibility condition* is satisfied. The reconstruction is possible by using the following reconstruction formula (*Inverse Wavelet Transform*):

$$x(t) = \frac{1}{C_\psi} \int \int CWT_x^\psi(\tau, s) \frac{1}{s} \psi \left(\frac{t - \tau}{s} \right) d\tau ds \quad (3.7)$$

Where, C_ψ is a constant that depends on the wavelet used. The success of the reconstruction depends on this constant called, *the admissibility constant*, to satisfy the following *admissibility condition*:

$$C_{\psi} = \left\{ 2\pi \int_{-\infty}^{\infty} \frac{|\widehat{\psi}(\xi)|^2}{|\xi|} d\xi \right\}^{1/2} < \infty \quad (3.8)$$

Where, $\widehat{\psi}(\xi)$ is the FT of $\psi(t)$. Equation (3.8) implies that, $\widehat{\psi}(0) = 0$, which is

$$\int \psi(t) dt = 0 \quad (3.9)$$

Equation (3.9) is not a very restrictive requirement since many wavelet functions can be found whose integral is zero. For equation (3.8) to be satisfied, the wavelet must be oscillatory [18].

3.3.4. Multi-Resolutional Approach (MRA)

Unlike STFT which has a constant resolution at all times and frequencies, WT uses a Multi-Resolutional Approach (MRA), i.e. varying temporal resolution for different spectral components, which can be clarified as follows. A lower or narrower scale (higher frequencies) means lesser ambiguity in time, i.e. good time resolution. Higher scales (lower frequencies) have wider support, leading to more ambiguity in time, or in other words, poor temporal resolution. The following figure compares the resolution for four different representations of the same signal.

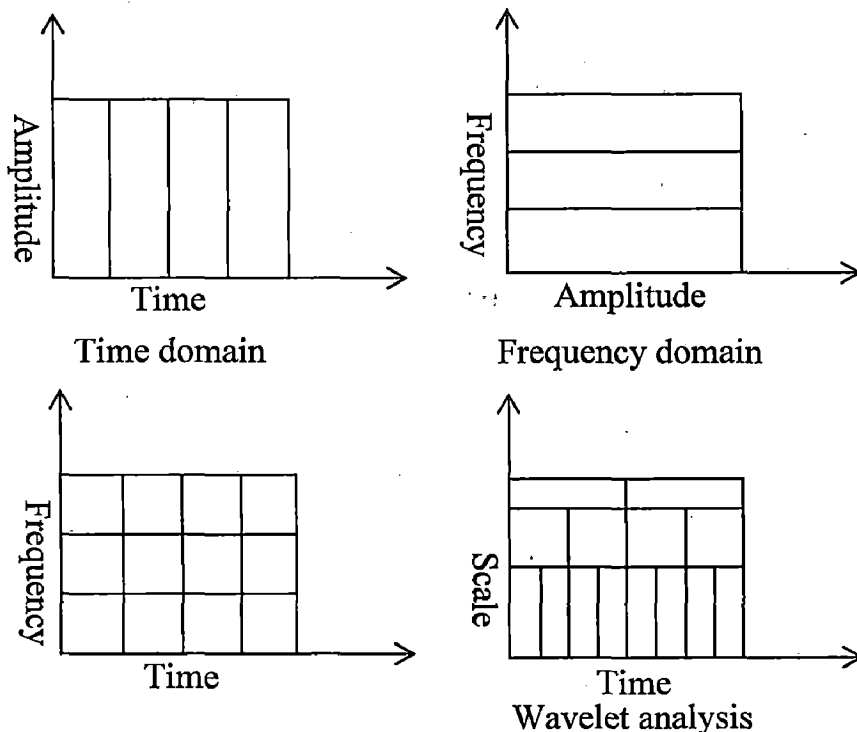


Fig.3.3. Time-Frequency resolution at different signal representations

The original time-domain signal has got no time resolution problem, since we know the value of the signal at every instant of time. In the Fourier transformed version, there is no resolution problem in the frequency domain, i.e. we know precisely what frequencies exist. Conversely, the frequency resolution in time domain and time resolution in Fourier domain are zero, since we have no information about them. For the two bottom diagrams, each box represents an equal area of the time-frequency plane, but different sized boxes giving different proportion to time and frequency.

All the boxes are of same size for STFT, i.e. the time and frequency resolutions are constant all over the time-frequency plane. For wavelet transform, at low frequencies (high scales), the height of the boxes are shorter (which corresponds to better frequency resolution, since there is less ambiguity regarding the value of the exact frequency), but their widths are longer (which correspond to poor time resolution, since there is more ambiguity regarding the value of the exact time). At higher frequencies (low scales), width of the boxes decreases, i.e. the time resolution gets better, and height of the boxes increases, i.e. the frequency resolution gets poorer.

3.3.5. *Sampling and the Discrete Wavelet Series*

In order for the Wavelet transforms to be calculated using computers the data must be discretised. A continuous signal can be sampled so that a value is recorded after a discrete time interval, if the Nyquist sampling rate is used then no information should be lost. With Fourier Transforms and STFT's the sampling rate is uniform but with wavelets the sampling rate can be changed when the scale changes. Higher scales will have a smaller sampling rate. According to Nyquist Sampling theory, the new sampling rate N_2 can be calculated from the original rate N_1 using the following:

$$N_2 = \frac{s_1}{s_2} N_1 \quad (3.10)$$

Where s_1 and s_2 are the scales. So every scale has a different sampling rate.

After sampling the Discrete Wavelet Series can be used, however this can still be very slow to compute. The reason is that the information calculated by the wavelet series is still highly redundant, which requires a large amount of computation time. To reduce computation a different strategy was discovered and Discrete Wavelet Transform (DWT) method was born.

3.3.6. Discrete Wavelet Transform (DWT)

Basically, the discrete wavelet transform is meant to handle discrete-time signals. The DWT is considerably easier to implement when compared to the CWT. The DWT provides sufficient information both for analysis and synthesis of the original signal, with a significant reduction in the computation time.

The foundations of DWT go back to 1976 when techniques to decompose discrete time signals were devised. In the case of DWT, time-scale representation of a digital signal is obtained using *digital filtering* techniques. The signal to be analysed is passed through filters with different cut-off frequencies at different scales. Wavelets can be realized by *iteration of filters with rescaling*. The resolution of the signal, which is a measure of the amount of detail information in the signal, is changed by the filtering operations, and the scale is changed by up-sampling and down-sampling (sub-sampling) operations.

The DWT is computed by successive low-pass and high-pass filtering of the discrete time-domain signal as shown in the following figure. This is called the *Mallat Algorithm* or Mallat-tree decomposition. Its significance is in the manner it connects the continuous time multiresolution to discrete time filters. The signal is denoted by the sequence $x[n]$, integer 'n' denoting the sample number. G_o and H_o are the low and high pass *Analysis filters* (filters used for decomposition) respectively. At each level, the high pass filter produces *detail* information $d[n]$, whereas, the low pass filter associated with scaling function produces coarse *approximations*, $a[n]$.

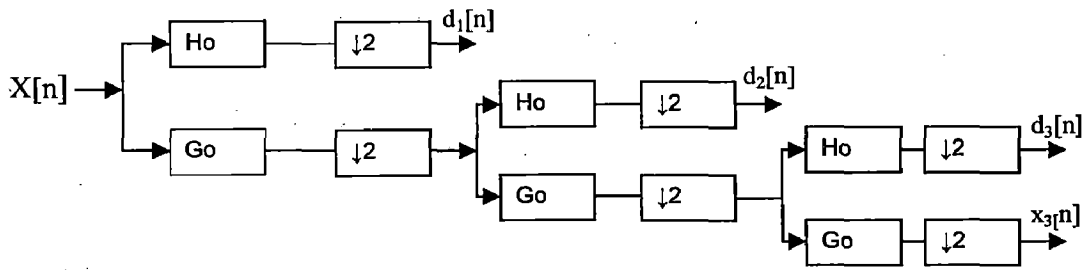


Fig.3.4 Three Level wavelet decomposition tree

At each decomposition level, the half band filters produce signals spanning only half the frequency band. This doubles the frequency resolution, as the uncertainty in frequency is reduced by half. According to *Nyquist's rule*, the sampling frequency of a signal needs to be at least double of its maximum frequency content in order to have a successful reconstruction. However, after each level of decomposition, the maximum frequency itself gets halved, and hence now its sampling frequency can also be reduced proportionally without any loss of information. This decimation by 2 halves the time resolution as the entire signal is now represented by only half the number of samples. This also doubles the scale.

The filtering and decimation process is continued until the desired level is reached. The maximum number of levels depends on the length of the signal. The DWT of the original signal is then obtained by concatenating all the coefficients, $a[n]$ and $d[n]$, starting from the last level of decomposition

3.3.7. Reconstruction of original time-domain signal from its DWT

The reconstruction is basically the reverse process of decomposition. The approximation and detail coefficients at every level are up-sampled by two, passed through the low pass and high pass *synthesis filters* (G_1 and H_1) and then added. This process is continued through the same number of levels as in the decomposition process to obtain the original signal. The Mallat Algorithm works equally well if the analysis filters, G_0 and H_0 , are exchanged with the synthesis filters, G_1 and H_1 .

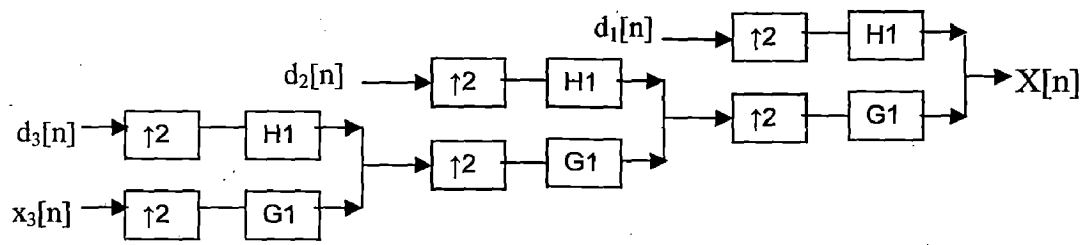


Fig.3.5. Three level wavelet reconstruction tree

CHAPTER-4

LUNG SOUND ANALYSIS

Over the last 30 yrs, computerized methods for the recording and analysis of respiratory sounds have overcome many limitations of simple auscultation. Respiratory acoustic analysis can now quantify changes in lung sounds, make permanent records of the measurements made and produce graphical representations that help with the diagnosis and management of patients suffering from chest diseases.

Respiratory sounds contain significant information on physiology and pathology of the lungs and the airways. The frequency spectrum and the amplitude of sounds, *i.e.* tracheal or lung sounds without adventitious sound components (crackles or wheezes), may reflect airway dimension and their pathologic changes (*e.g.* airway obstruction) or pathologic changes in the pulmonary tissue.

Sounds generated in healthy lungs and airways by normal breathing, differ according to the location where they are recorded and vary with the ventilatory cycle. The origin of sounds generated by ventilation is not completely clear. The lung itself cannot generate sound if there is no airflow; pressure differences between structures within the thorax or different lung volume levels cannot by themselves induce sounds in the absence of airflow. Breath sounds are probably induced by turbulence of the air at the level of lobar or segmental bronchi. In smaller bronchi, the gas velocity decreases and becomes less than the critical velocity needed to induce turbulence. Therefore, the airflow in smaller airways is believed to be laminar and silent.

The resulting noise, coming from the larger airways, has a wide frequency spectrum. It is transmitted to the skin, after filtering by the lungs and the chest wall, which act acoustically as a low-pass filter. Therefore, the nominal breath sounds recorded over the lungs have their main frequency band up to 200–350 Hz. Unfortunately this frequency band also contains components from respiratory muscles and the heart.

When recorded over the trachea, the sound is not (or less) filtered. Therefore, and also due to resonance phenomena, the frequency spectrum contains higher frequency components as high as 1200 Hz [19].

4.1. Frequency Domain Analysis

4.1.1. Analysis with Fourier Transform

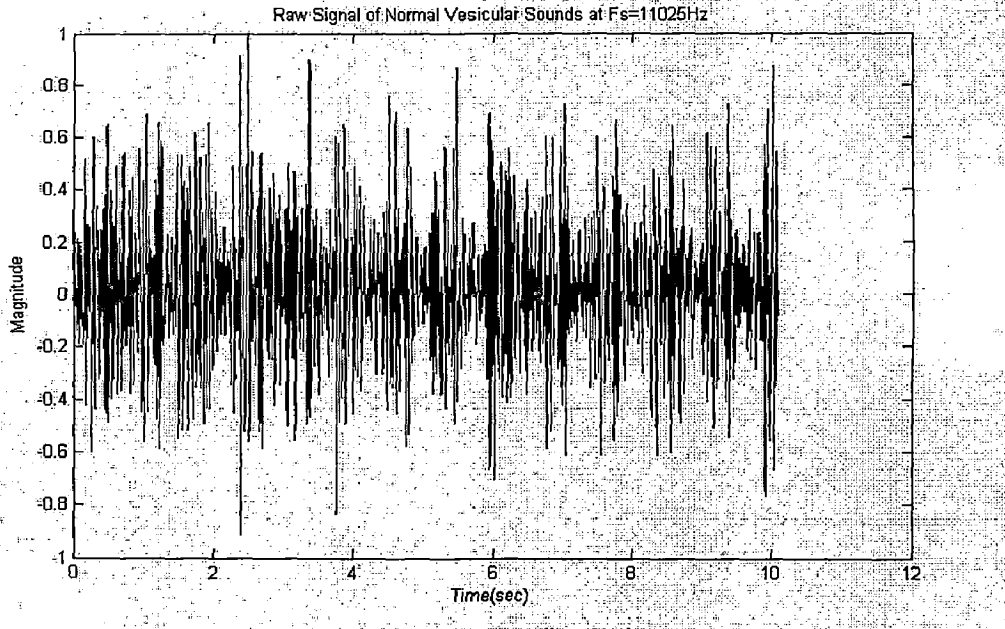


Fig.4.1 Raw signal of normal vesicular sounds

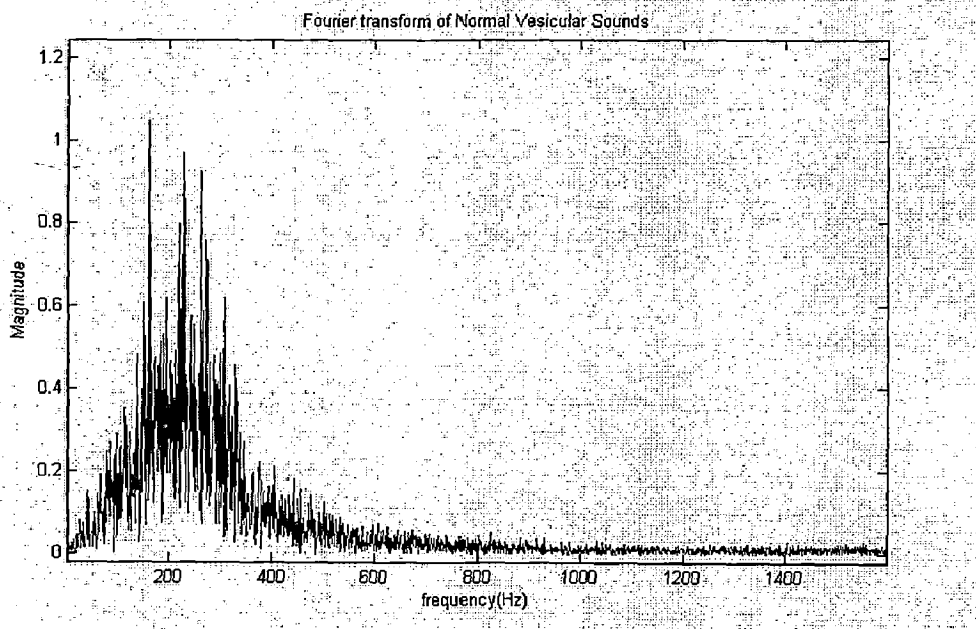


Fig.4.2 Fourier transform of normal vesicular sounds.

4.1.2. Analysis with STFT

Similar to Fourier Transform, the short time Fourier transform is invertible. The short time Fourier transform satisfies the linearity, time shift, frequency shift properties on similar lines with the Fourier transform.

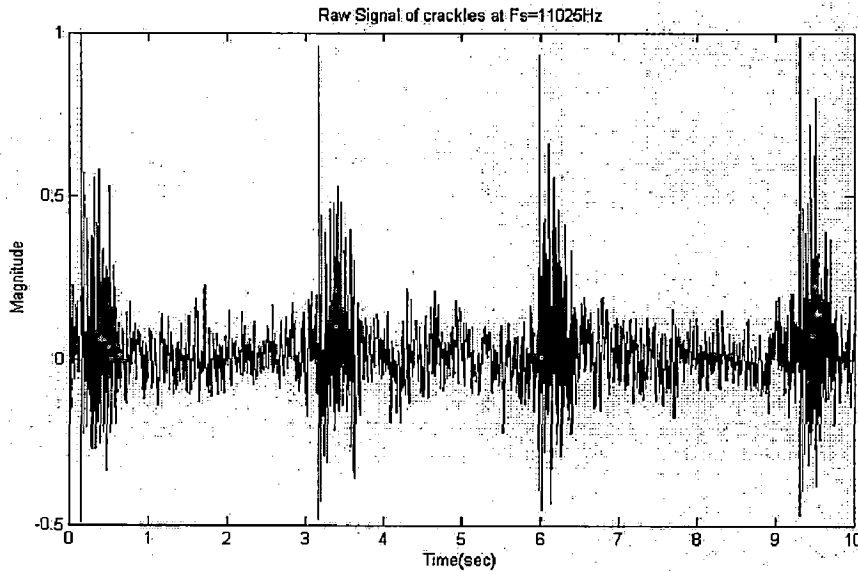


Fig.4.3 Raw signal of crackles

Above raw signal is having nonstationary characteristics so this signal is better analyzed using any Time-Frequency analysis technique. Here i used a Hanning window of 256 samples.

Hanning Window

The coefficients of a Hann window are computed from the following equation

$$w[k+1] = 0.5 \left(1 - \cos \left(2\pi \frac{k}{n-1} \right) \right), \quad k=0, \dots, n-1; \quad (4.1)$$

Fig.4.4..shows a hann window of 256 samples with its frequency response.

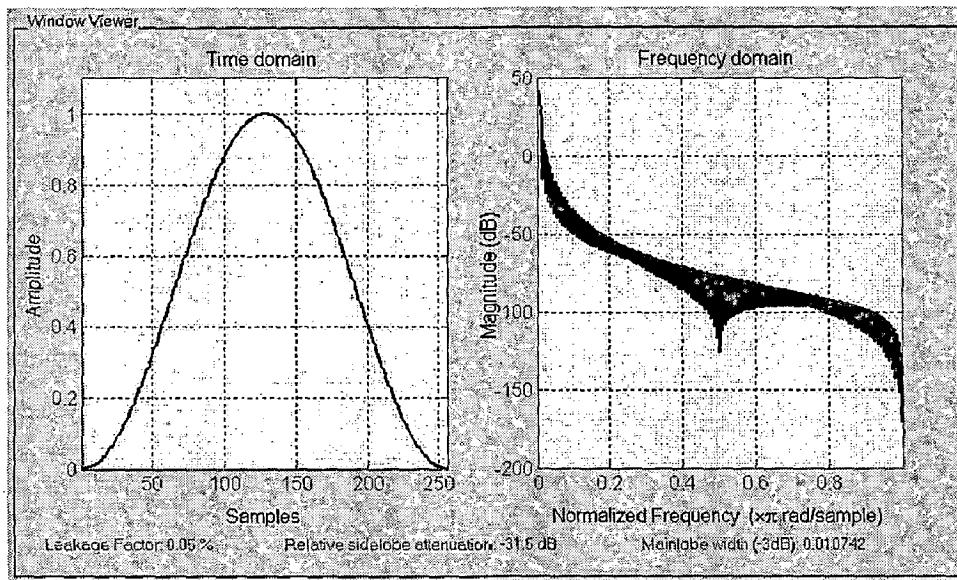


Fig.4.4 Hanning window of 256 samples.

Using this window STFT was done on crackles and resulting frequency information with its time and amplitudes were represented in 3D plot as shown in Fig.4.5.

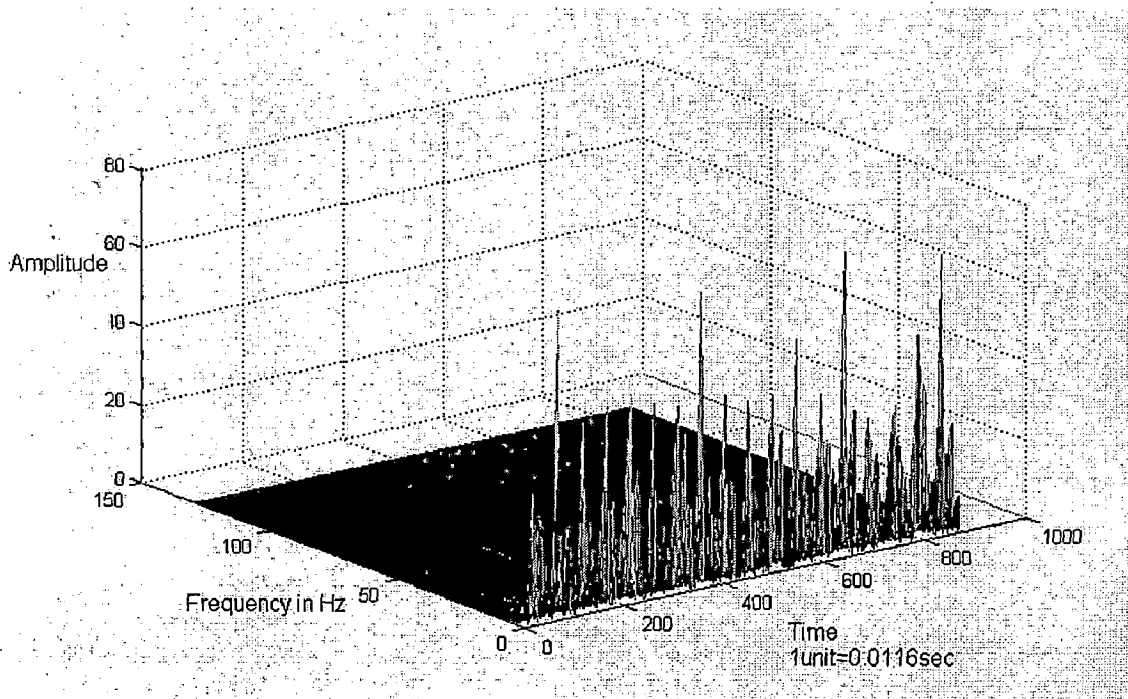


Fig.4.5 Spectrogram of crackles.

4.1.3. Analysis With Wavelet Transform

Here in the analysis using wavelets i used daubechies (db10) and biorthogonal (bior3.7) as mother wavelets, they were taken by considering the shape of crackles, wheezes and other adventitious sounds. In the following figures Normal and other adventitious sounds are detected by decomposing the raw signals which are recorded at sampling frequency $F_s=11025$ Hz to a level where these sounds are clearly visible (where more energy is concentrated). Required signal components are present in the frequency range 650 to 150 Hz for the most of signals [8].

Normal Vesicular Sounds

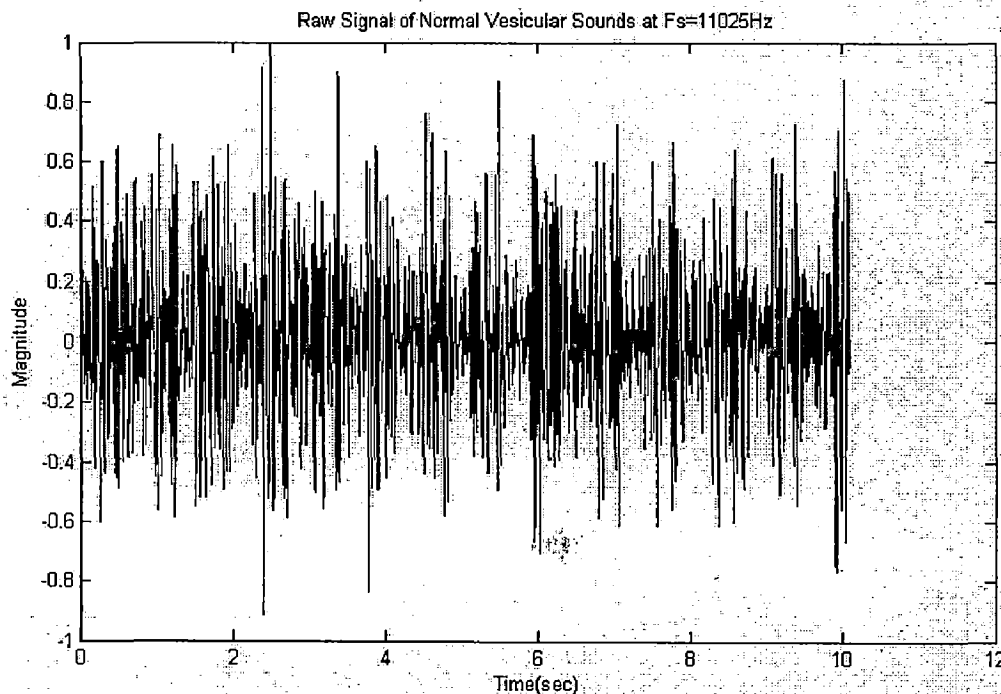


Fig.4.6 Raw signal of sampling frequency (F_s):11025Hz

This raw signal is decomposed using wavelet db10. At the 5th level in the frequency range 625-312 Hz normal inspiration and expiration periods are identified. Inspiratory period is longer than the expiratory period. Fig 4.7 shows these periods.

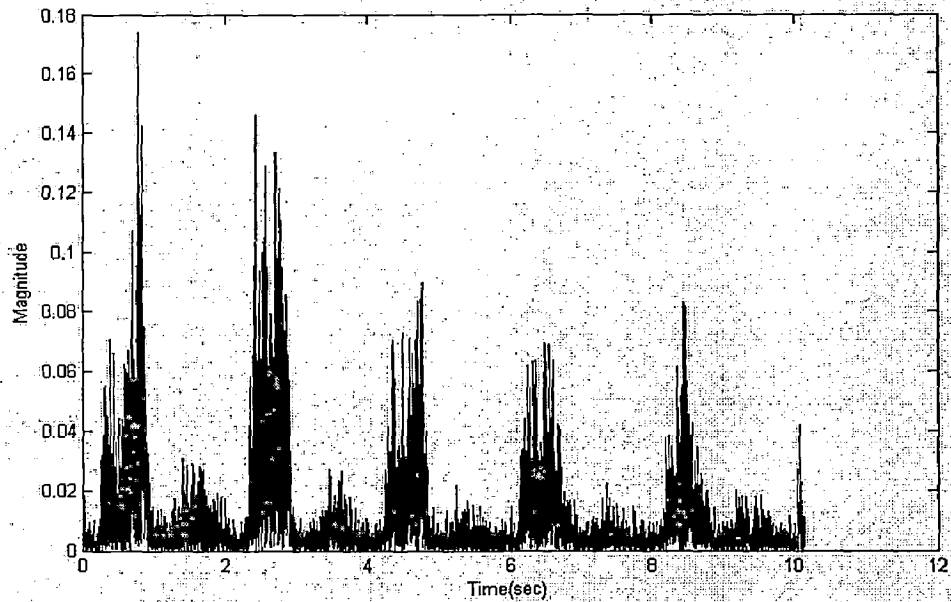


Fig.4.7 Inspiratory and Expiratory periods of normal lung sounds

Lung Sounds with Crackles

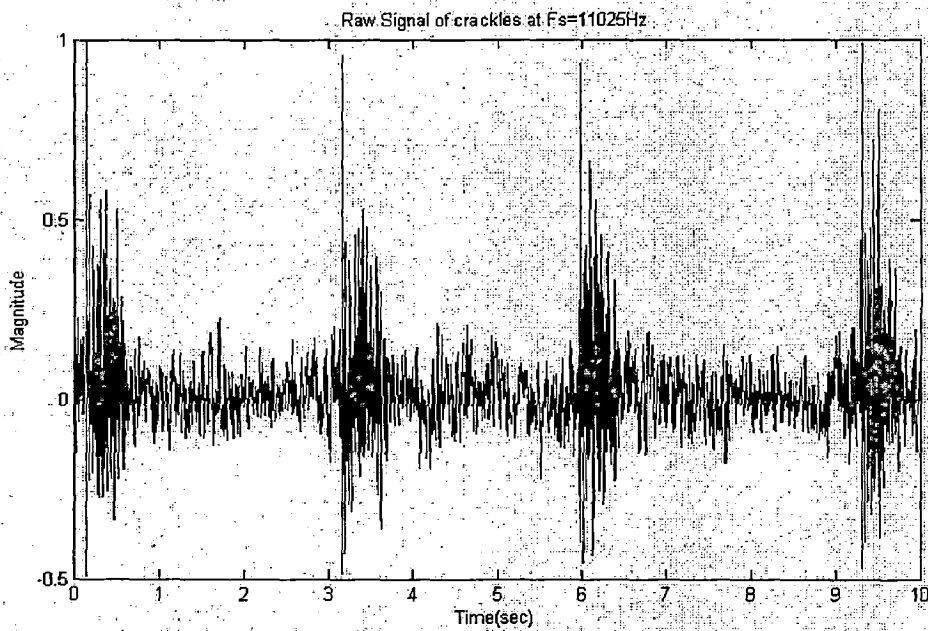


Fig.4.8.Raw signal of lung sounds with crackles

By considering the shape of crackles as shown in fig.4.9 i selected biorthogonal wavelet-3.7.After decomposing up to 5th level (625-312Hz) required crackles are identified as shown in Fig.4.10 [7].

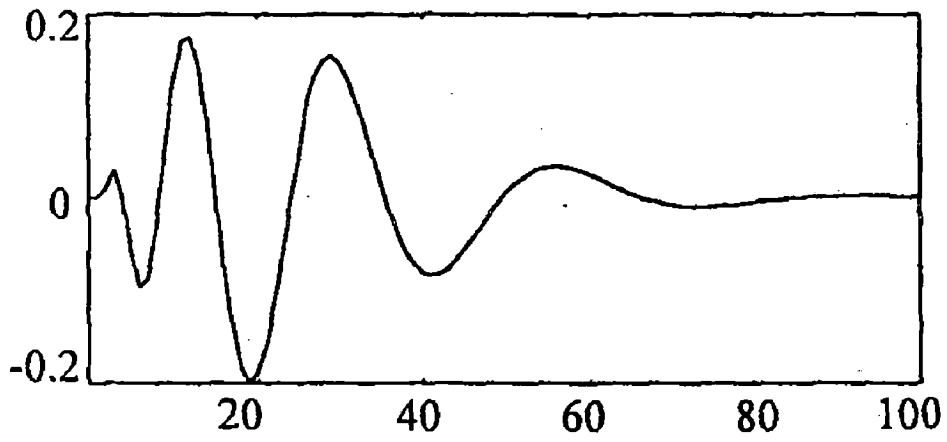


Fig.4.9 An ideal crackle

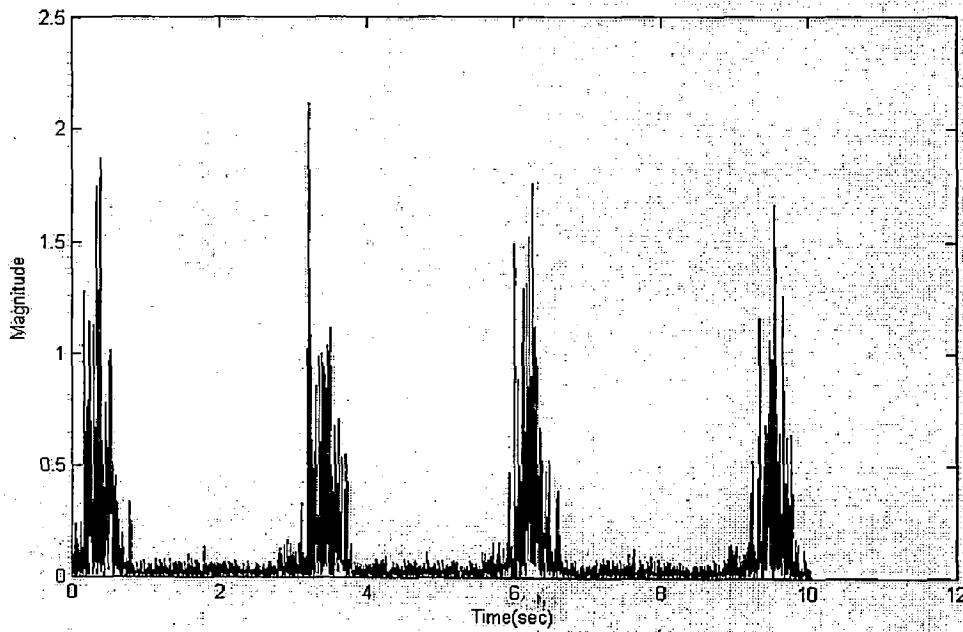


Fig.4.10 Identified crackles in 5th level of decomposition

Lung sounds with Wheezes

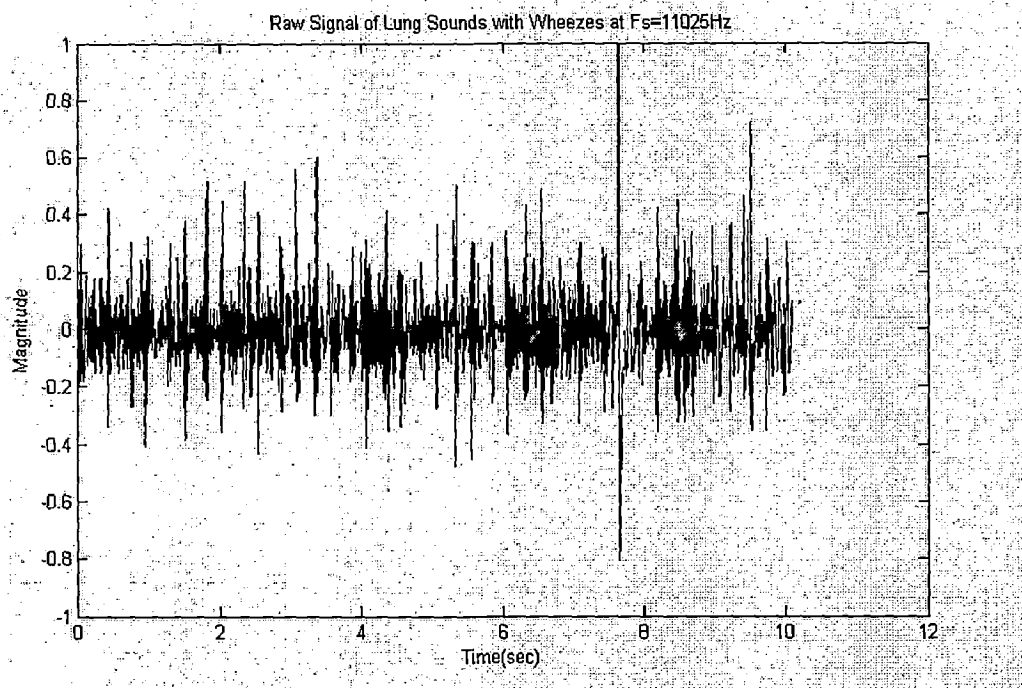


Fig.4.11 Raw signal of lung sounds with wheezes

After decomposing to 5th level the identified wheezes [11] are as shown in Fig.4.12.

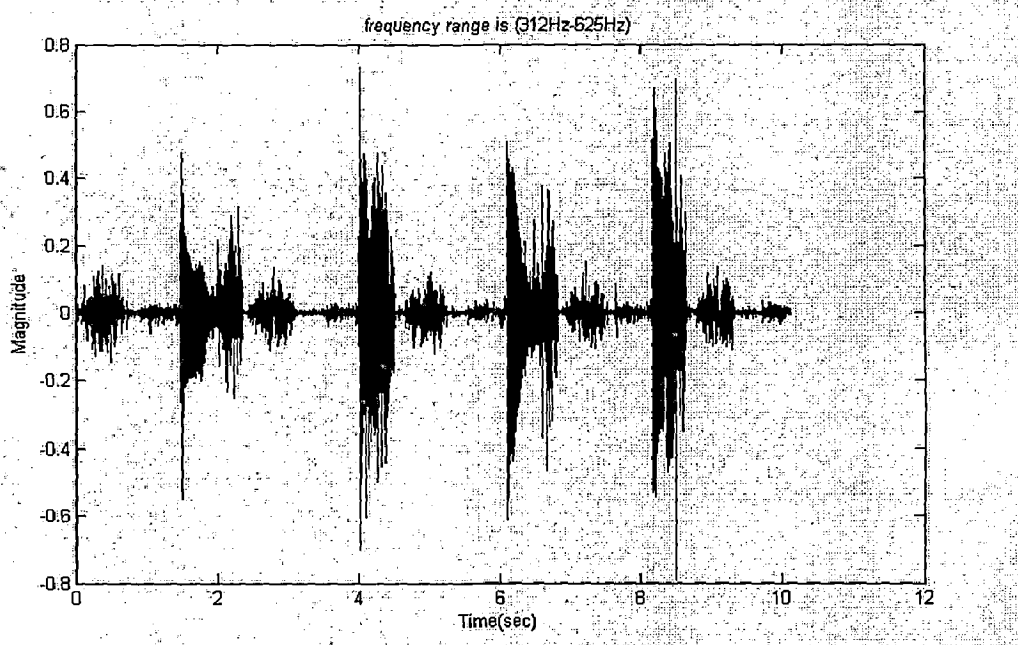


Fig.4.12 Identified wheezes

4.2. Separation of Fine Crackles from Vesicular Sounds By Nonlinear Digital Filter

Crackles are discontinuous adventitious lung sounds explosive and transient in character, and occur frequently in cardio respiratory diseases. Their duration is less than 20 ms, and their frequency content typically is wide, ranging from 100 to 2000 Hz or even higher. Two types of crackles may be distinguished: coarse and fine. Crackles are assumed to originate from the acoustic energy generated by pressure equalization or a change in elastic stress after a sudden opening of abnormally closed airways [10].

These crackles present in lung sounds in various diseases and reason for generation of these sounds is different in these diseases:

- In cardiorespiratory disorders where crackles are frequently found, abnormal closure of the small airways may result from increased elastic recoil pressure (*e.g.* in pulmonary fibrosis) or from a stiffening of small airways caused by accumulation of exudated fluid (*e.g.* in heart failure) or infiltrative cells (*e.g.* pneumonitis, alveolitis).
- The mechanisms of generation of the crackling sounds in chronic bronchitis and emphysema are incompletely understood, but, bubbling of air through secretions is one possible mechanism but does not account for all the crackling phenomena in these patients.
- When present, crackling sounds in patients with lung fibrosis are typically fine, repetitive, and end inspiratory, whereas those associated with chronic airways obstruction (*e.g.* emphysema or bronchiectasis) are coarse, less repeatable, and occur early in inspiration.
- Patients with airways obstruction may also have expiratory crackles, and, unlike in patients with pulmonary fibrosis, the crackles may be audible at the mouth; in addition, these crackles may change or disappear after coughing. In heart failure, the crackles tend to occur from the mid to late inspiratory cycle, and they are coarse in character.

Mathematical models and experiments predict that crackles originating from smaller airways are shorter in duration (fine in character), and those originating from larger airways are more coarse.

Crackles are one of the most important physical signs in clinical medicine. Since crackles are discontinuous and nonstationary signals, time-domain analysis is mandatory where detection and/or separation of the individual crackle signal is the most fundamental process. High-pass filters have been used but the separation is incomplete and the waveforms are distorted by this method. The application of a level slicer is limited because the amplitude of fine crackles is often small.

So far, the most accurate method is a visual approach using the time-expanded waveform analysis. It is, however, time consuming and the interobserver variability is inevitable. Therefore, it is desirable to establish a more efficient and objective method. With this in mind we applied a nonlinear digital filter to the separation of crackles from vesicular sounds

4.2.1. The Stationary-Nonstationary Separating Filter

The nonlinear digital filter we used was designed for separating nonstationary from stationary signals, and is called stationary-nonstationary separating filter (ST-NST filter). Suppose that the input signal (X_n) is a summation of two types of signals: the stationary signal which can be expressed by an autoregressive model and the nonstationary signal composed of random impulsive waves whose occurrence rate is low.

Under these circumstances we can separate nonstationary from stationary signals using the stationary-nonstationary separating filter which is constructed as shown in Fig.4.14.

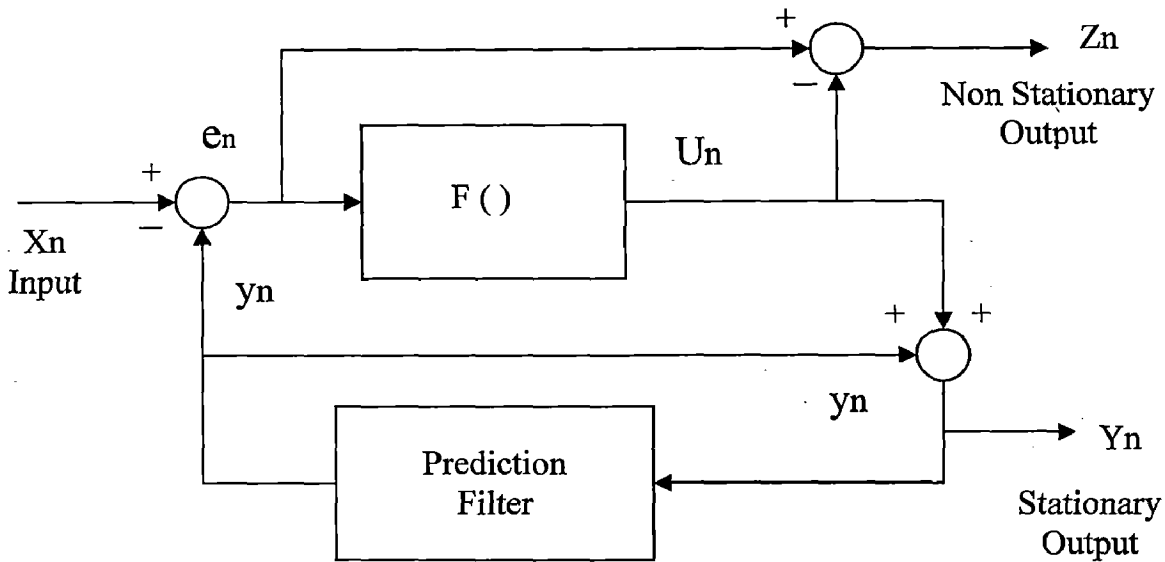


Fig.4.13 Schematic diagram of ST-NST filter

Where X_n , is the input, Z_n is the nonstationary output, and Y_n is the stationary output. The prediction filter performs autoregressive prediction using the estimated stationary waves Y_n as follows:

$$Y_n = \sum_{k=1}^M a_k y_{n-k} \quad (4.2)$$

Here a_k represents the coefficients of the autoregressive model, and M the order of it. In this work, the coefficients are set adaptively by an LMS algorithm. The prediction error (e_n) for the input X is obtained, and is processed by $F()$ for determining U_n which is the part included in the stationary component, as follows:

$$e_n = X_n - y_n \quad (4.3)$$

$$U_n = F(e_n) \quad (4.4)$$

Here $F(\cdot)$ is a nonlinear function defined as in Fig.4.14 where \mathcal{E} is determined so that the probability of detection of nonstationary waves is given by certain value γ where

$$\int_{-\mathcal{E}}^{+\mathcal{E}} p(x) dx = 1 - \gamma \quad (4.5)$$

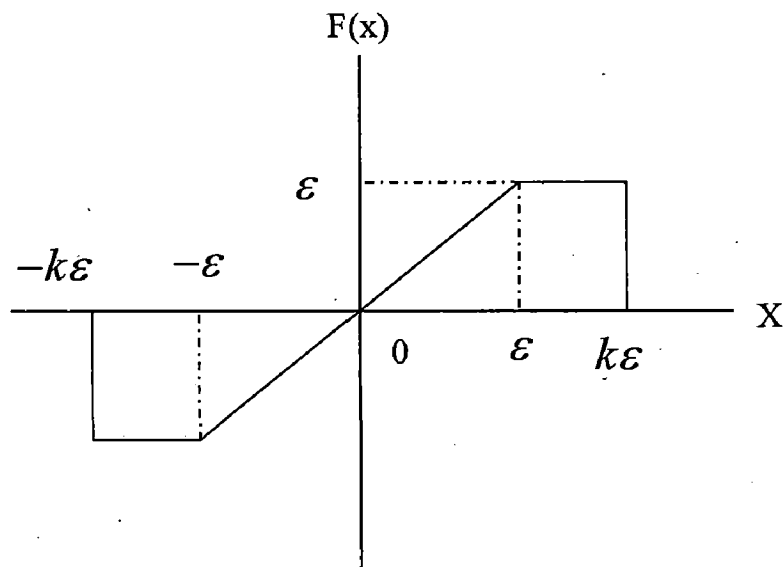


Fig.4.14 Definition of non linear function.

Values of M , k are taken as 15 and 2 and value of Σ depend up on prediction error. Here $p(x)$ is the probability density function of the prediction error of the original signal and is assumed here to be nearly Gaussian. Finally, Z_n (the nonstationary output) and Y_n , (the stationary output) are obtained as follows:

$$Y_n = y_n + U_n \quad (4.6)$$

$$Z_n = e_n - U_n \quad (4.7)$$

4.2.2. Least Mean Square Algorithm

LMS algorithm was implemented to get the prediction filter coefficients (a_k) in Fig.6.1. Many adaptive algorithms can be viewed as approximations of these discrete filter as shown in Fig.4.16

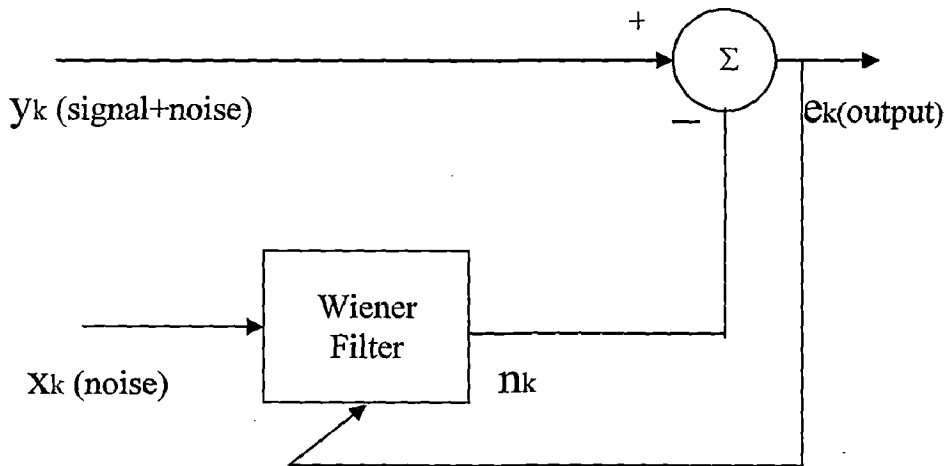


Fig.4.15 The basic wiener filter

The wiener filter produces an optimal estimate of part of y_k that is correlated with x_k which is then subtracted from y_k to yield e_k . Assuming FIR structure with N coefficients (weights) the error, e_k , between the wiener filter output and the primary signal, y_k , is given by [18]

$$e_k = y_k - n_k = y_k - W^T X_k = y_k - \sum_{i=0}^{N-1} w(i) x_{k-i} \quad (4.8)$$

Where X_k and W , the input signal vector and weight vector, respectively, are given By:

$$X_k = \begin{bmatrix} x_k \\ x_{k-1} \\ \vdots \\ \vdots \\ x_{k-(N-2)} \\ x_{k-(N-1)} \end{bmatrix} \quad W = \begin{bmatrix} w(0) \\ w(1) \\ \vdots \\ \vdots \\ w(N-2) \\ w(N-1) \end{bmatrix} \quad (4.9)$$

square of error is given as:

$$e_k^2 = y_k^2 - 2y_k X_k^T W + W^T X_k X_k^T W \quad (4.10)$$

MSE (J) is obtained by expectations of both sides of equation.4.10.

$$J = E[e_k^2] = E[y_k^2] - 2E[y_k X_k^T W] + E[W^T X_k X_k^T W] \quad (4.11)$$

$$\text{and} \quad \nabla = \frac{dJ}{dW} = -2P + 2RW \quad (4.12)$$

Where $P = E[y_k X_k]$ and $R = E[X_k X_k^T]$

$$W_{opt} = R^{-1}P \quad (4.13)$$

In LMS the coefficients are adjusted from sample to sample in such a way as to minimize the MSE (mean square error).The LMS is based on the steepest descent algorithm where the weight vector is updated from sample to sample as follows:

$$W_{k+1} = W_k - \mu \nabla_k \quad (4.14)$$

The widrow-Hopf LMS algorithm for updating the weights from sample to sampl is given by

$$W_{k+1} = W_k + 2\mu e_k X_k \quad (4.15).$$

4.2.3. Implementation of basic LMS algorithm

The computation procedure of the LMS algorithm is summarized as follows:

1. Initially, set each weight $w_k(i)$, $i=0, 1 \dots N-1$, to an arbitrary fixed value, such as 0

For each subsequent sampling instant, $k=1,2,\dots$, carry out steps (2) to (4) below.

2. Compute filter output
$$n_k = y_k - \sum_{i=0}^{N-1} w(i)x_{k-i}.$$

3. Compute the error estimate

$$e_k = y_k - n_k$$

4. Update the next filter weights

$$w_{k+1}(i) = w_k(i) + 2\mu e_k x_{k-i}.$$

By training I found filter coefficients ($N=15$) and by using these coefficients in Fig.6.1.I got the stationary output (with out crackles) and nonstationary output (crackles) for different samples of lung sounds [5].

4.2.4. Results

Sample 1

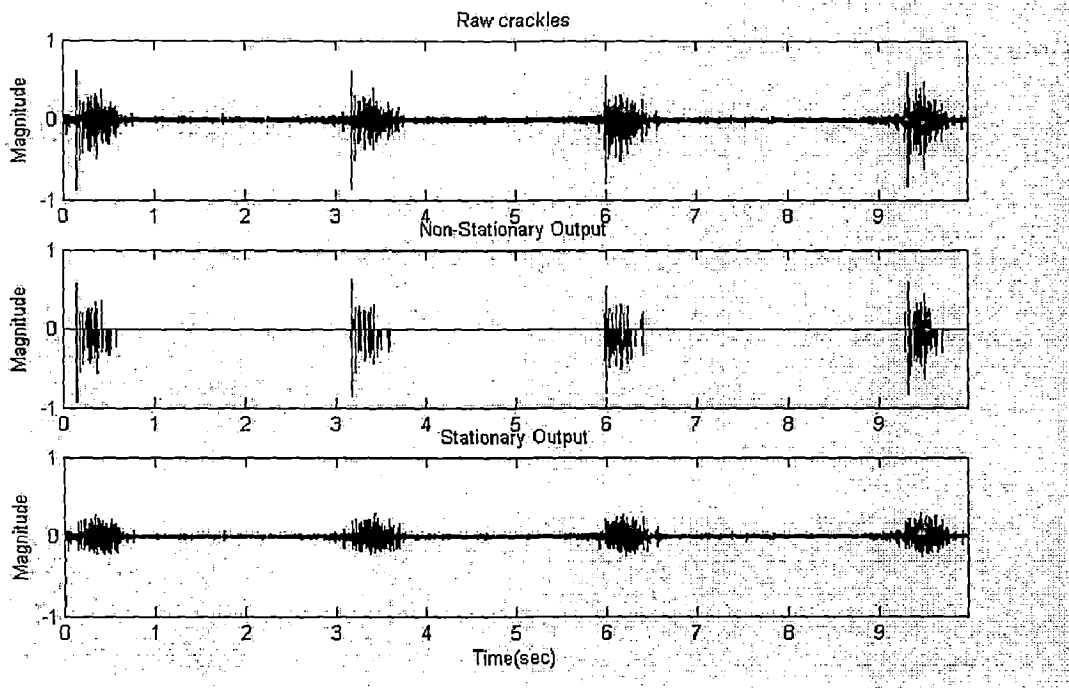


Fig.4.16 Raw crackles with separation of crackles.

In the Fig.4.16 We clearly saw the crackles separated from the raw signal which are nonstationary in nature.

Sample 2

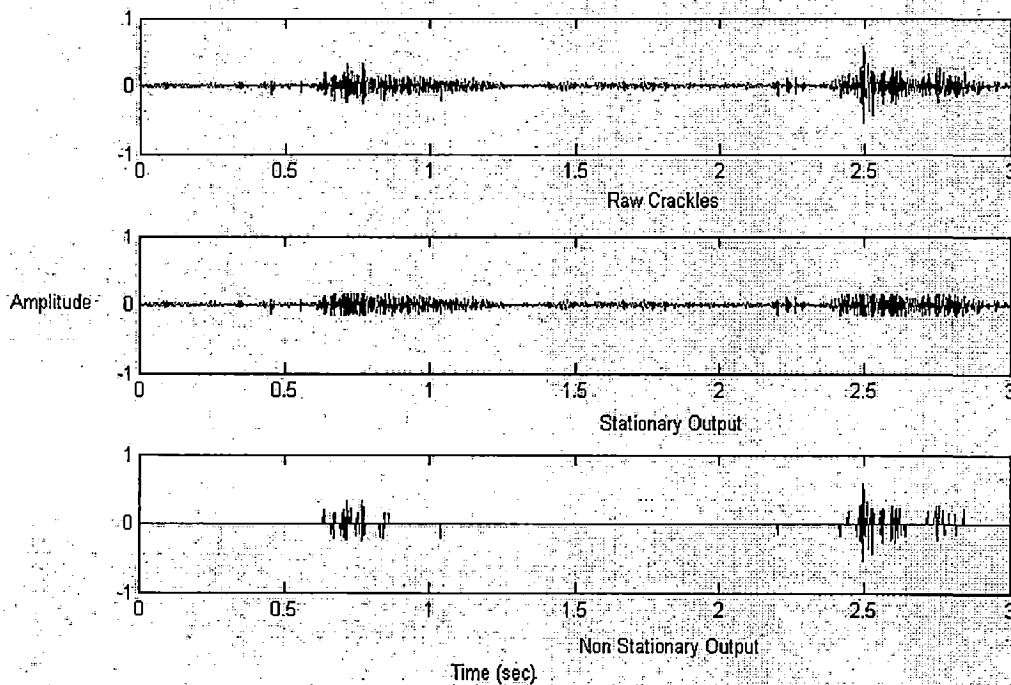


Fig.4.17 Raw crackles with separation of crackles for sample2

Sample 3

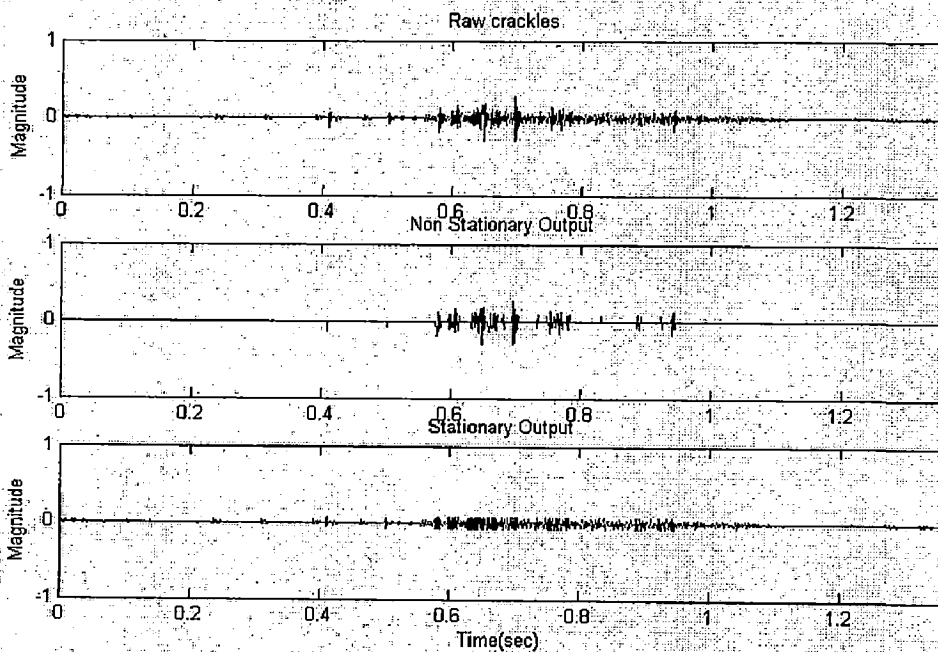
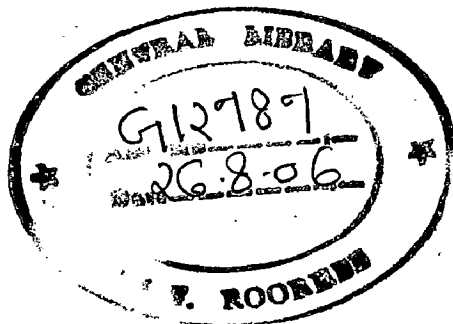


Fig.4.18 Raw crackles with separation of crackles for sample3



4.3. Wheeze Episode Detector Using DWT

Wheezes are continuous adventitious lung sounds, which are superimposed on the normal breath sounds. The waveform of a wheezing sound resembles that of a sinusoidal sound. According to the earlier definition of the American Thoracic Society (ATS), the word "continuous" means that the duration of a wheeze is longer than 250ms. Wheeze contains a dominant frequency of 400 Hz or more. According to the new definitions of the present CORSA (Computerized Respiratory Sound Analysis) guidelines, the dominant frequency of a wheeze is usually >100 Hz and the duration >100 ms. Wheezes, which are louder than the underlying breath sounds, are often audible at the patient's open mouth or by auscultation by the larynx.

The transmission of wheezing sound through the airways is better than transmission through the lung to the surface of the chest wall. The higher-frequency sounds are more clearly detected over the trachea than at the chest. The high-frequency components of breath sounds are absorbed mainly by the lung tissue.

Wheezes can be heard in several diseases, not only in asthma. They are common clinical signs in patients with obstructive airways diseases, and particularly during acute episodes of asthma. There is no relationship between the pitch of wheezes and the pulmonary function. The appearance and quantification of wheezes have also been used for the assessment of bronchial hyper responsiveness in bronchial-challenge tests. Wheezes are very often reported by patients who wake up at night with nocturnal asthma symptoms. Thus, a non-invasive monitoring of wheezes has been proposed to assess changes in airways obstruction during sleep, without disturbing the patient.

4.3.1 Wheeze Episode Detector

The most straightforward methods for automatic wheezing detection are based on searching for peaks in successive spectra. The algorithms that are used in these studies are quite simple and fast, however, they are not very reliable, since they exhibit quite low sensitivity. Recent attempts for achieving higher sensitivity accompanied with efficient detection performance include a set of criteria in the time-frequency domain. These criteria refer to time duration, pitch range and magnitude of wheezes in their time-frequency representation by means of their spectrogram analysis.

Discrete Wavelet Transform (DWT) is used to form a DWT-based Wheezing-Episode Detector (DWT-WED). In this way, the DWT-WED takes into account the beneficial properties of the DWT representation over the Fourier one, since, unlike the latter, the DWT provides useful information regarding the coherent nature of the localized features within the signal, such as wheezing episodes.

This method is structured twofold. In particular, it not only focuses in identifying the true location of the wheezes within the breathing cycle, but it also aims at separating the wheeze signal from the acquired lung sound. In this way, the diagnostic character of the wheeze is unveiled, since its contamination due to the superimposition of the breathing sound is circumvented. As a result, the CWT-WED acts both as an identification and denoising tool.

4.3.2. Wheeze Identification

In particular, the N- sample acquired lung sound signal, $x(k)$, can be considered as the sum of an envelop confined sinusoidal signal of interest, $s(t)$, i.e., wheezes, and the breathing sound, $n(k)$, (seen here as a kind of background noise) hence, it can be written as:

$$x(k) = s(k) + n(k), k=1 \dots N \quad (4.16)$$

By using DWT raw lung sound signal with wheezes is decomposed and in the range of 625-312Hz frequency these wheezes are detected. For some of signals these are identified in the range of 312-150Hz frequencies. For decomposing i used Daubechies-

10(db10) as mother wavelet. Explanation about the wavelet analysis (CWT and DWT) was already discussed in earlier of this chapter [13].

The sample of wheezes shown in below Fig.4.18 is recorded at sampling frequency 22 kHz .And it is decomposed by DWT using db-10 wavelet and 5th level (315-150Hz) wheezes are dominated compare do other levels as shown in fig.4.19.

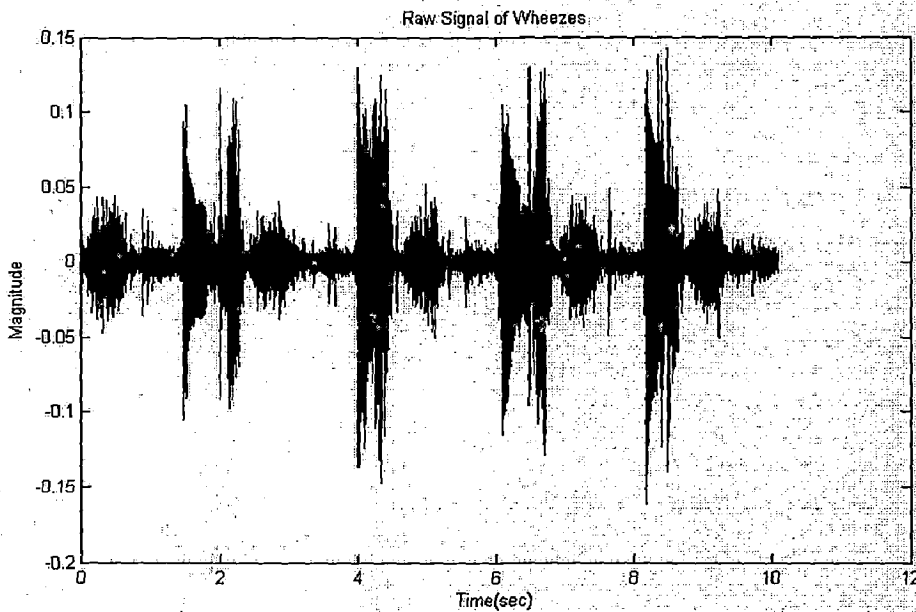


Fig.4.19 Raw signal of wheezes

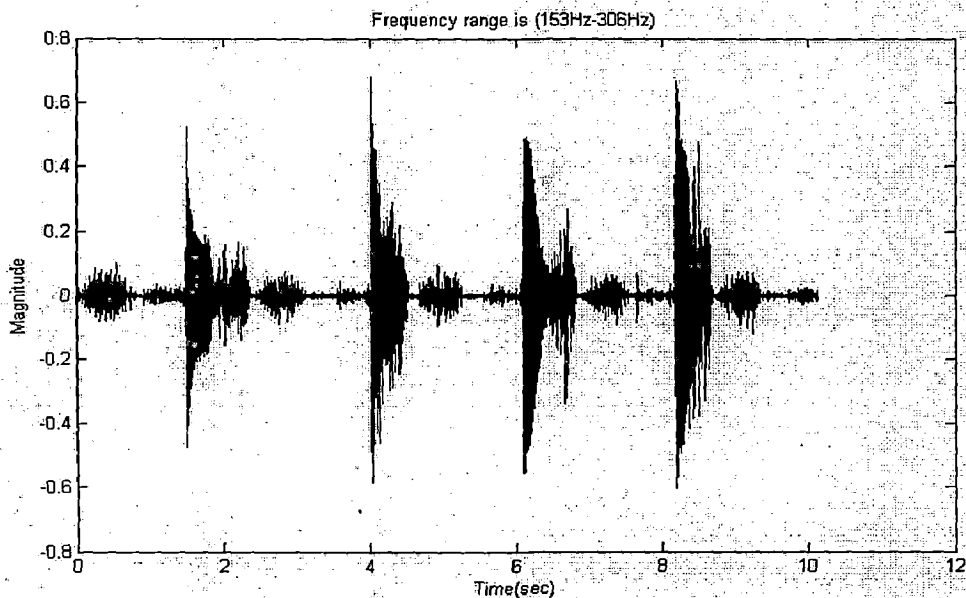


Fig.4.20 Identified wheezes

4.3.3. Wheeze Denoising

The denoising performance of the DWT-WED is achieved by applying frequency-dependent thresholding. This helps to the reduction of the high and low frequency noise components in the reconstructed signal. Due to the localization of the DWT both in time and frequency, the reconstructed signal resembles the output of an adaptive filtering, retaining the desired structural characteristics only at the true locations of the signal of interest $s(t)$ [13].

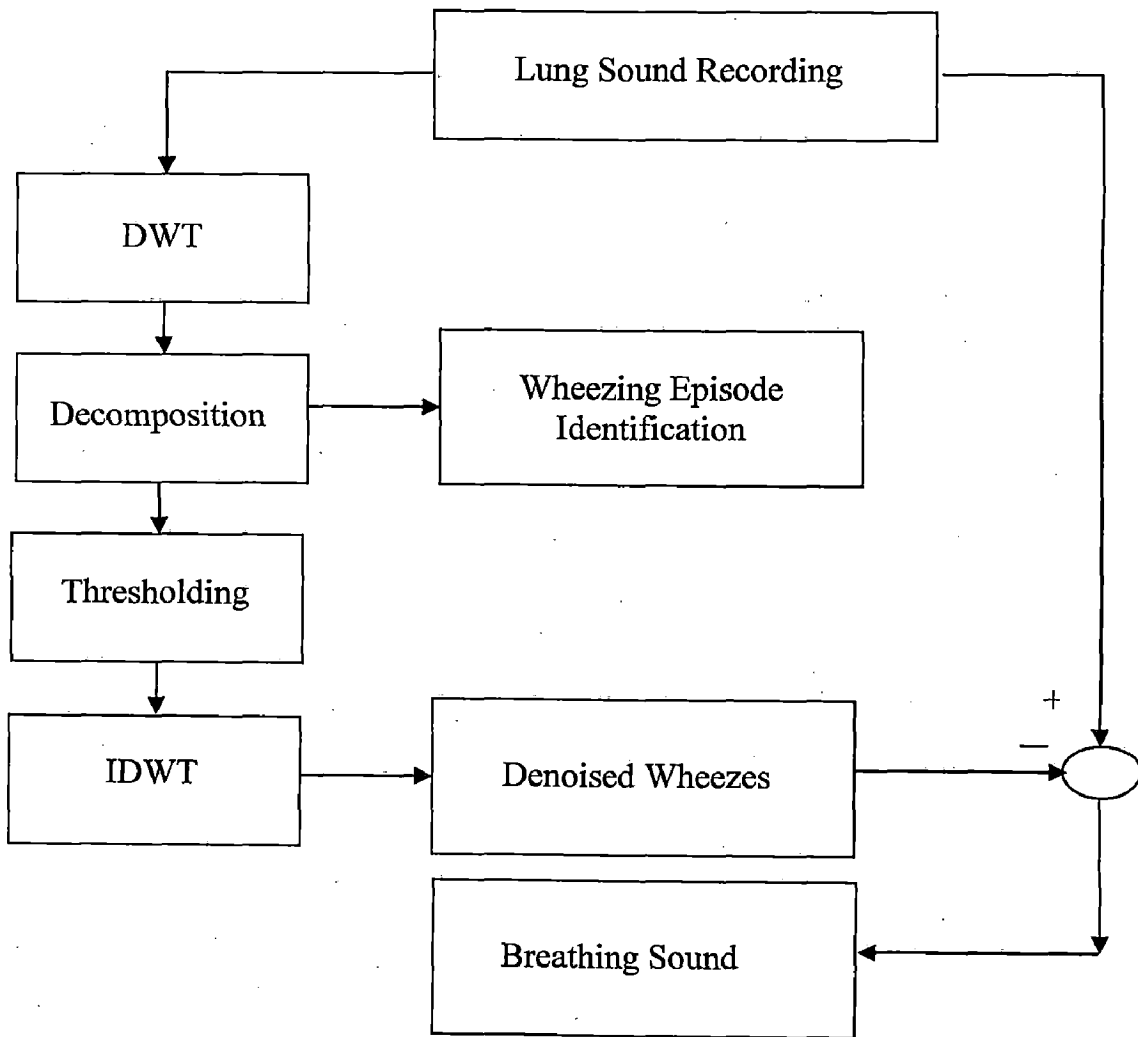


Fig.4.21.Simplified block diagram of DWT-WED scheme

Recorded lung sound signal is initially filtered and decomposed using DWT and wheezes are detected at particular frequency level at that instant wheezes are dominant compared to other components present. So by using thresholding criteria detected wheezes are separated (noise) from the signal at that level and the signal reconstructed from that level by using IDWT and breath sounds are displayed with out wheezes.

For the above sample shown in figure 4.19 after denoising these are resulted waveforms:

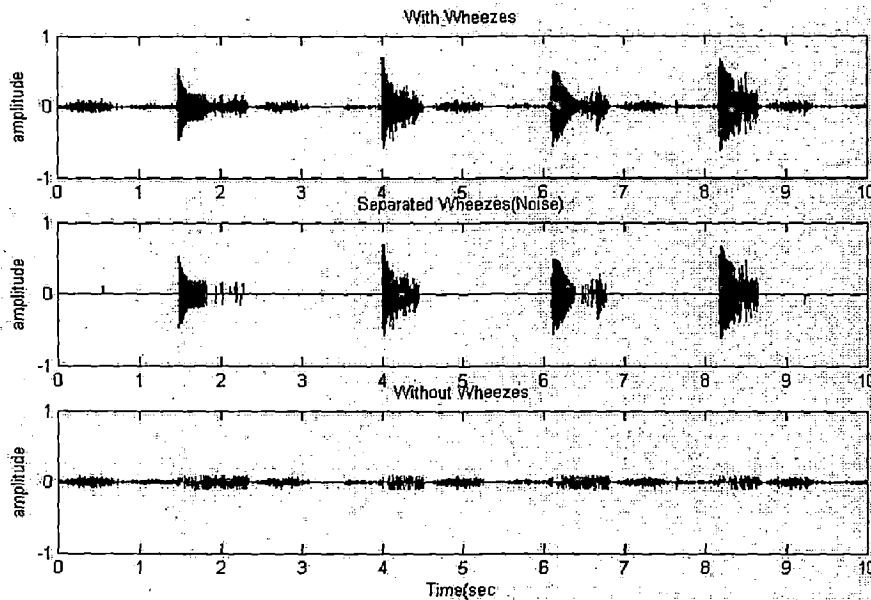


Fig.4.22 Separated wheezes from breath sound

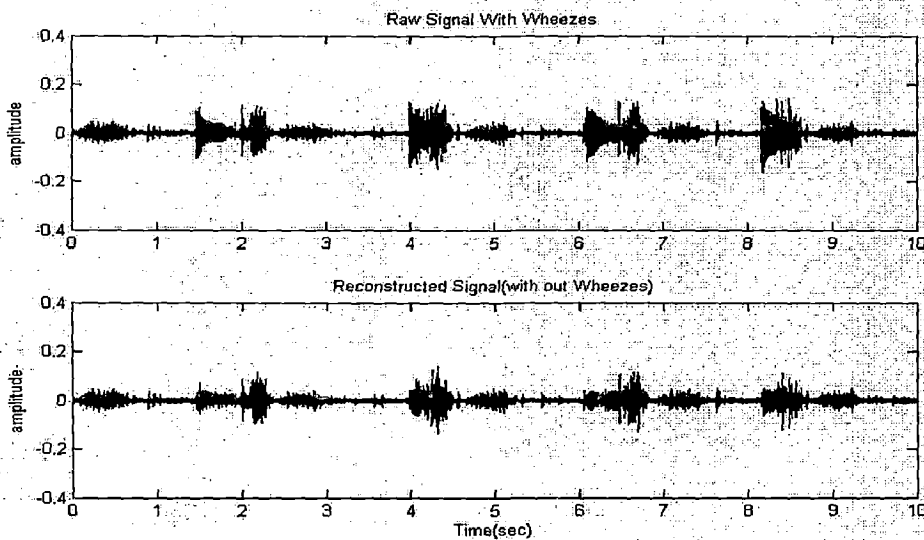


Fig.4.23 Original and reconstructed signal (without wheezes)

4.3.4. Results

Sample 1 results are discussed earlier with analysis.

Sample2

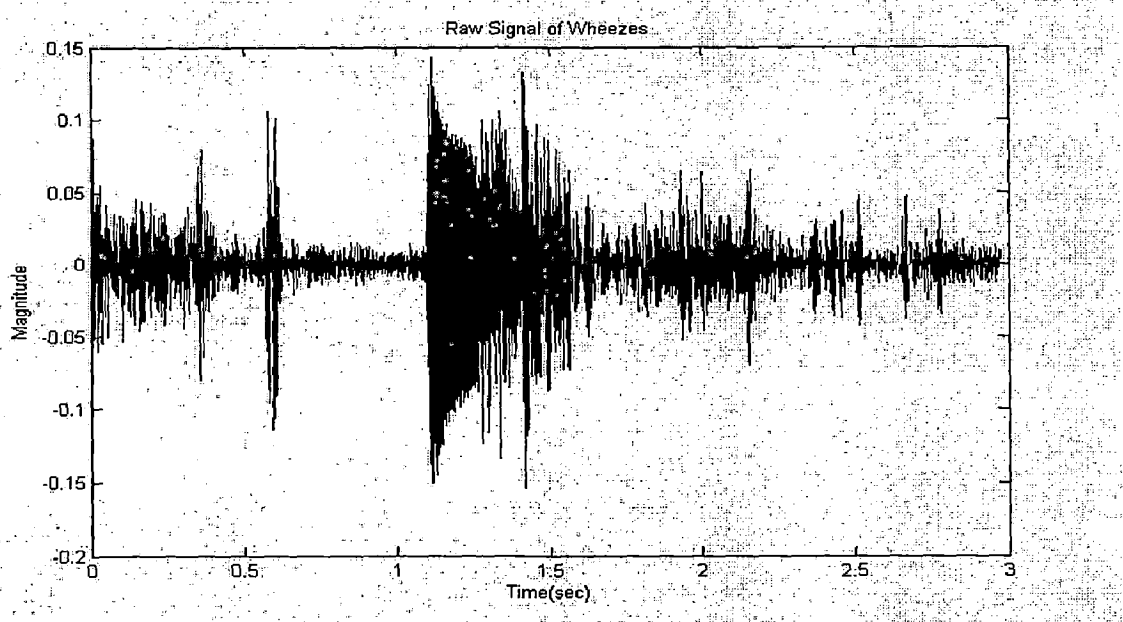


Fig.4.24 Raw signal with wheezes

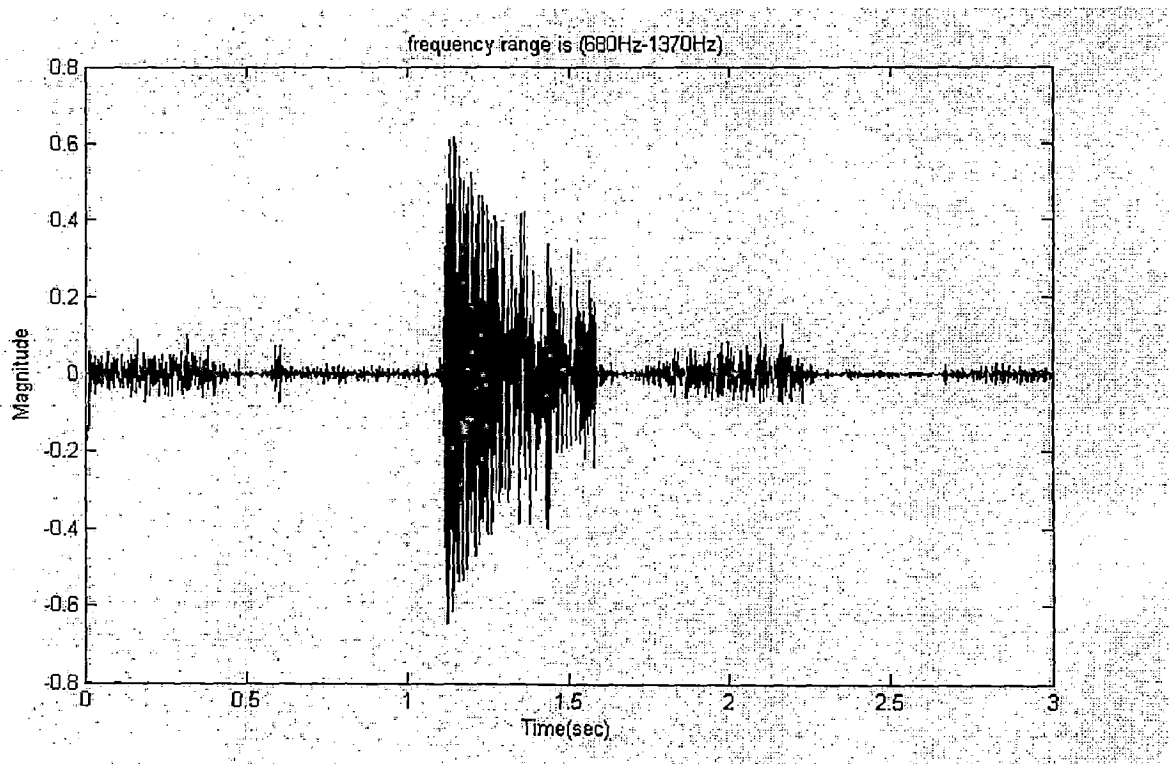


Fig.4.25 Detected wheezes after decomposition

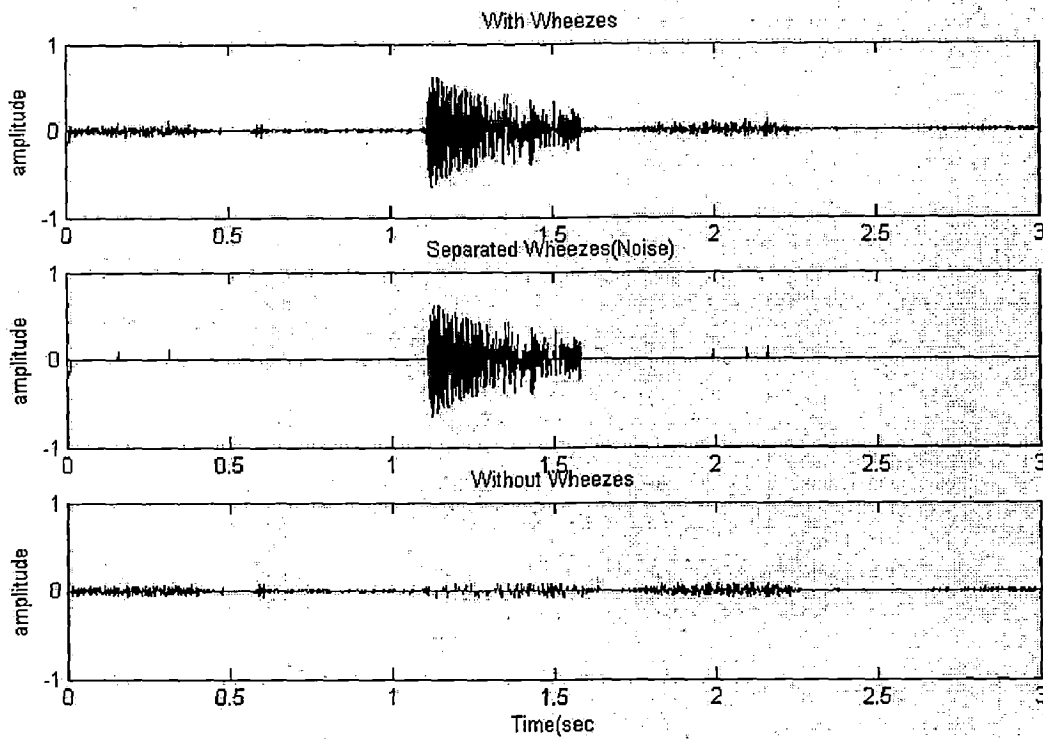


Fig.4.26 Separated wheezes from breath sounds

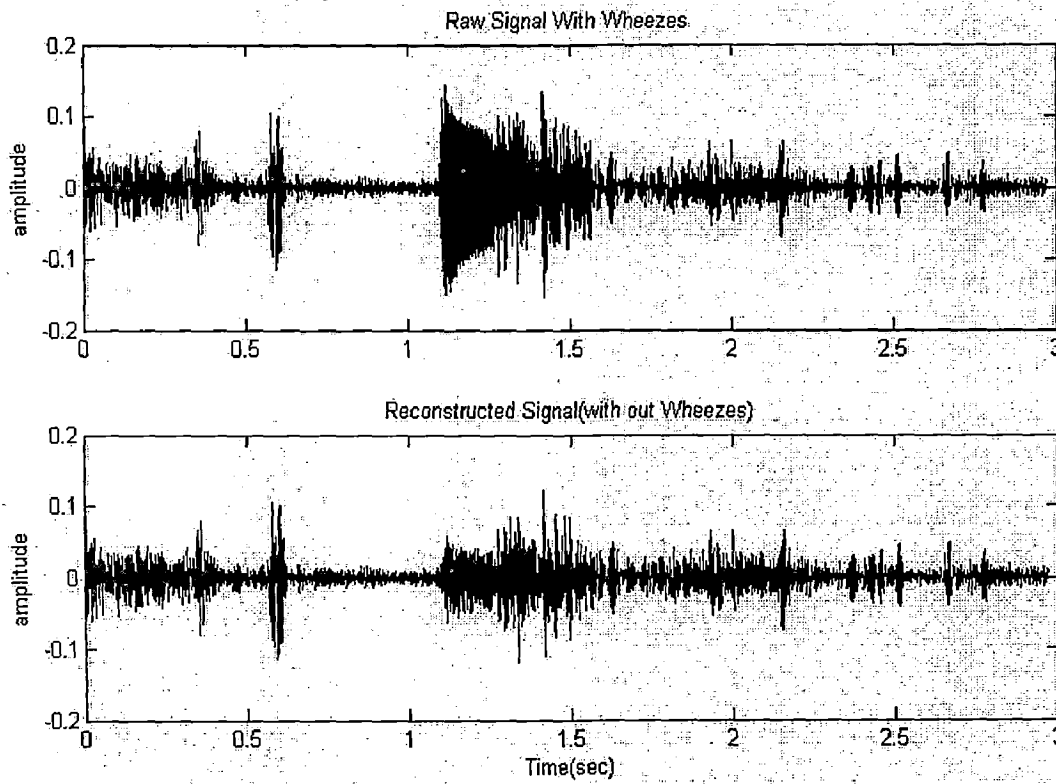


Fig.4.27 Raw signal and reconstructed signal (without wheezes)

Sample3

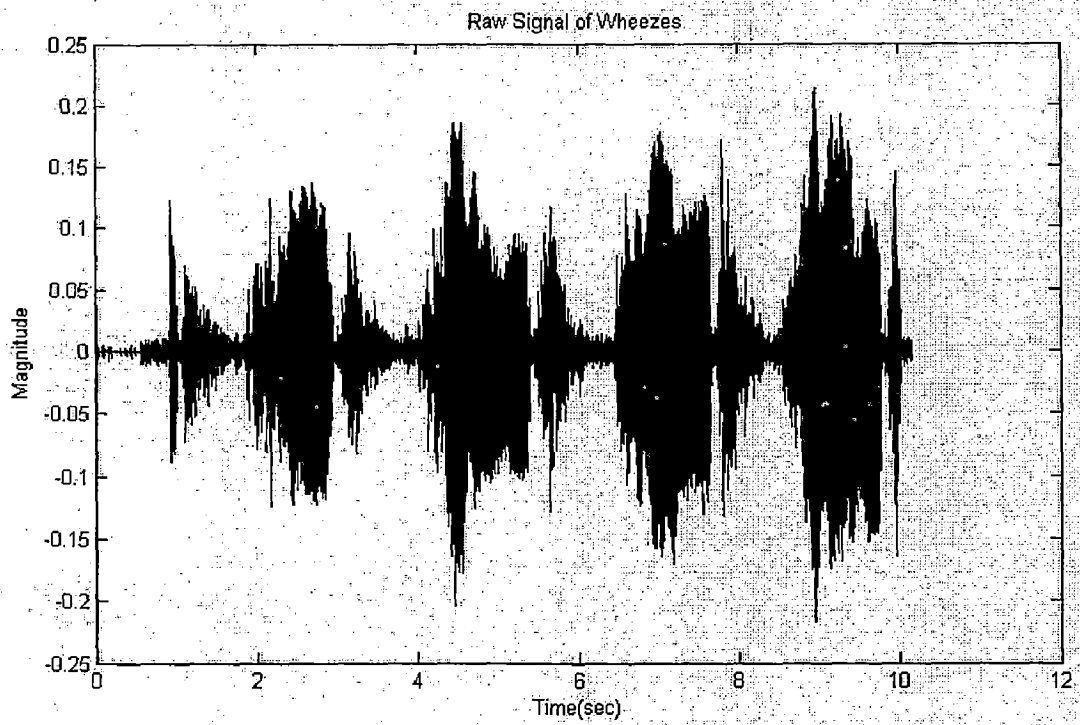


Fig.4.28 Raw signal with wheezes

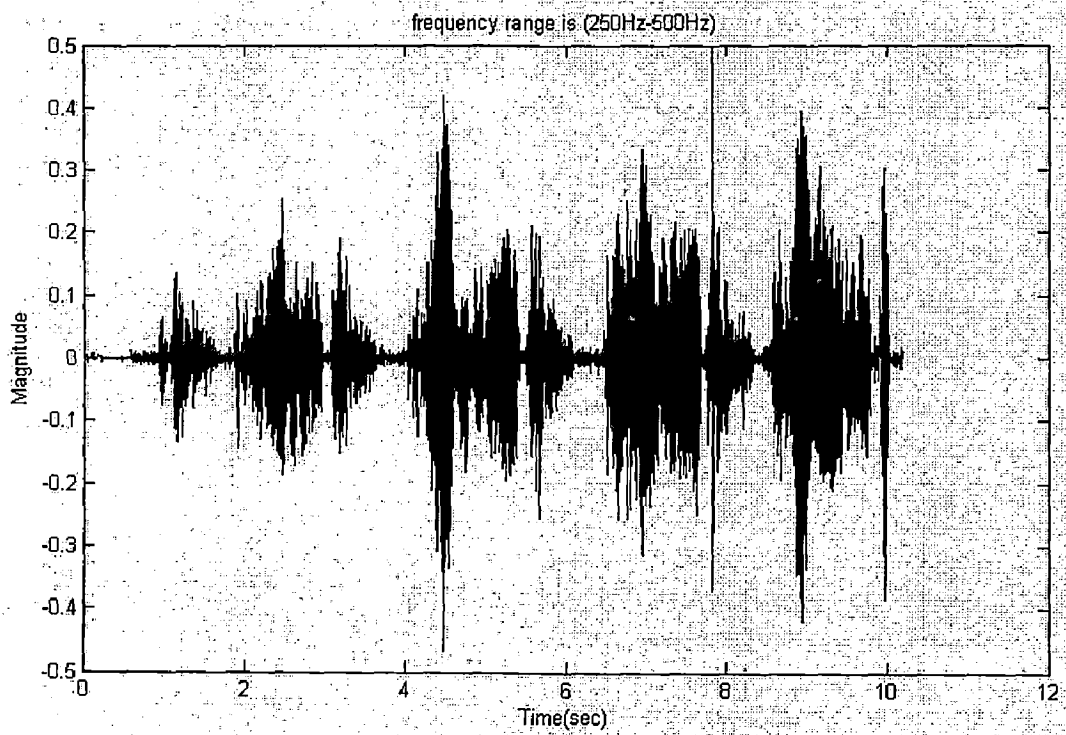


Fig.4.29 Detected wheezes after decomposition

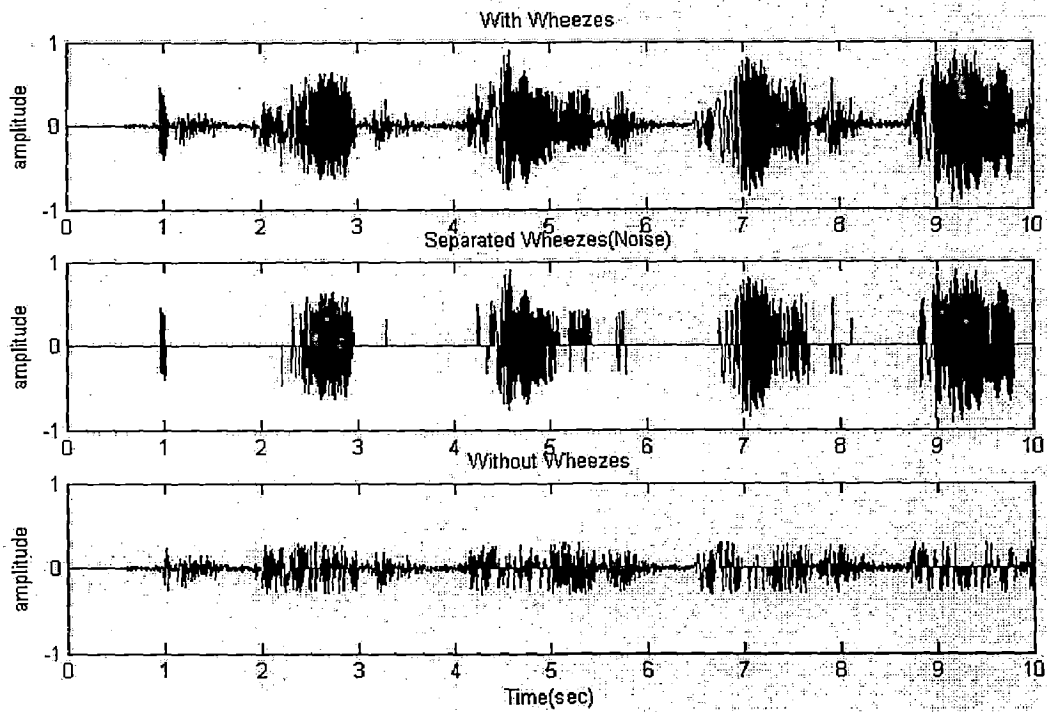


Fig.4.30 Separated wheezes from breath sounds

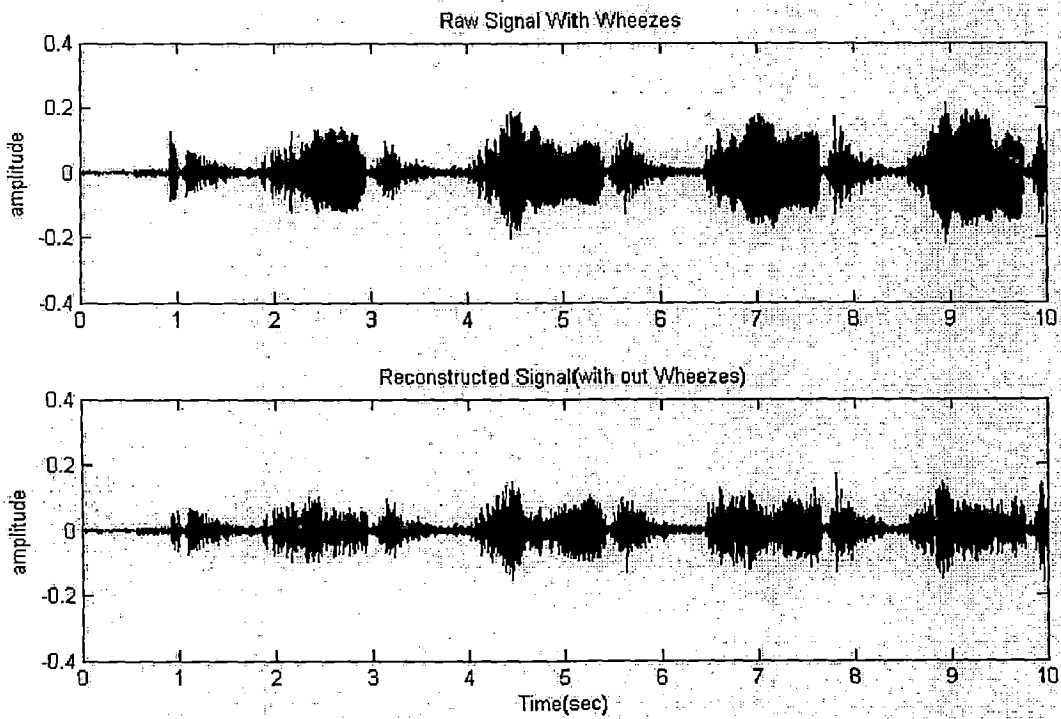


Fig.4.31 Raw signal and reconstructed signal (without wheezes)

4.4. Heart Sound Reduction in Lung Sounds by Spectrogram

It is rarely possible to obtain recordings of lung sounds that are 100% free of contaminating sounds from nonrespiratory sources, such as the heart. Depending on pulmonary airflow, sensor location, and individual physiology, heart sounds may obscure lung sounds in both time and frequency domains, and thus pose a challenge for development of semi-automated diagnostic techniques.

The turbulence involved with the movement of air through the respiratory airways is the predominant mechanism responsible for the generation of basic lung sounds. Chest-surface lung sounds have been used for the indication and diagnosis of underlying physiological conditions since the invention of the stethoscope. It has been shown that the intensity of breath sounds increases with increasing airflow; however, the time and frequency domain combination of sounds originating from pulmonary airflow with sounds from heart and muscle in signals acquired on the chest wall, complicates the definition of flow-specific lung sounds as a function of underlying airway conditions for diagnostic purposes.

A few researchers have employed adaptive filtering schemes for reducing heart sounds in lung sounds recordings using recursive least squares (RLS) filtering, as well as least mean squares (LMS) filtering, Reduced order kalman filtering (ROKF), and a fourth order statistics filtering technique. However, a preferred signal processing method for this purpose has not been established.

The signal was filtered to remove DC with 8th order Butterworth band-pass filter with pass band 7.5Hz - 2500Hz then .The original sampling rate was 11025Hz.

4.4.1. Heart Sound Localization by Spectrogram

Time-frequency (TF) representations such as the spectrogram are specifically designed to process non-stationary signals as they jointly display time and frequency information demonstrating which frequencies occur at a certain time, or, at which times a certain frequency occurs. Spectrogram is computed by the windowed discrete-time Fourier transform of a signal using a sliding window and therefore sometimes called Short Time Fourier Transform (STFT). The function of the window is to extract a portion of the signal by ensuring that the extracted section is approximately stationary. The decrease of the window length increases the time resolution property of the spectrogram (wideband spectrogram) whereas the frequency resolution increases with an increase in window length (narrowband spectrogram). In this work i used a short window length (25ms-256 sample Hanning window) with 50 % overlap was used to calculate the Spectrogram. The reason of using short time period for spectral analysis is that high time resolution is beneficial to detect the heart sounds in the spectrogram [17]. Spectrogram of signal recorded at trachea of $F_s=11.025$ KHz is as shown in figure.4.31.

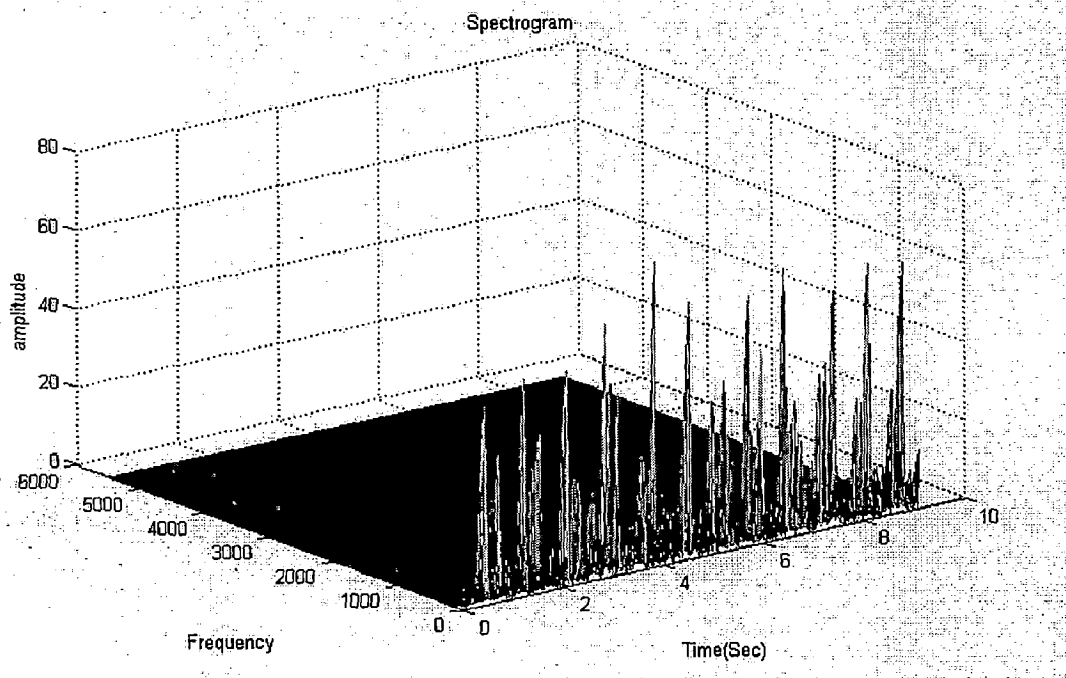


Fig.4.32 Spectrogram of lung Sounds with heart sounds

From the figure.4.32. It's clearly visible that in the low frequency range around 40-60Hz there large peaks. These peaks resemble heart sounds which are dominant compared to other components of lung sounds. High energy spikes of the heart sound signals can be localized by applying a threshold. Here threshold was chosen to be 20 after the examining the spectrum of the signal at 40-60Hz. Reference signal for heart sounds is formed by making samples as zeros which not up to the threshold and reconstruct the signal by using IFFT(IFFT is explained in earlier of this chapter).

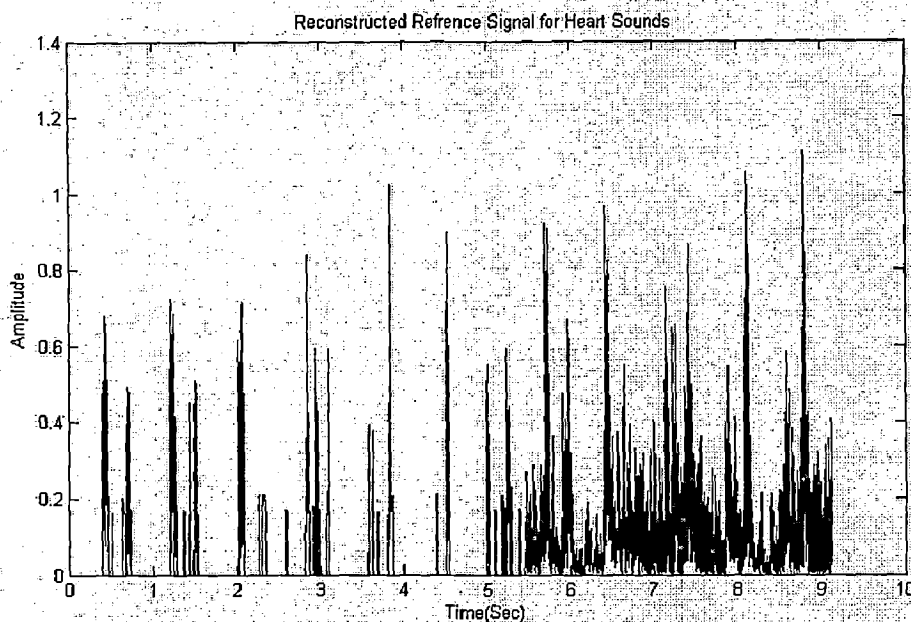


Fig.4.33 Reference signal for heart sounds

4.4.2. Heart Sound Filtering by RLS-ANC Adaptive Filter

The standard RLS adaptive filtering scheme consists of a transversal filter with finite-duration impulse response (FIR) and an RLS adaptation algorithm, which updates the tap, weights w_k of the transversal filter so that the mean square error (MSE) is minimized and an estimate of the desired output results. The RLS scheme was implemented in software, employing the method of least squares in a recursive manner.

Fig.4.34. depicts the specific configuration in which the general RLS filter was used in this work for ANC (Adaptive Noise Canceller). As shown in Fig.4.34. The algorithm accepts two input vectors: a reference and a primary input. The primary signal, $x(n)$, contains an interference, $m(n)$, alongside an information bearing signal component, $b(n)$, and the reference signal, $r(n)$, represents a version of the primary input with a weaker essentially undetectable information-bearing component. Reference data is arranged in an M-by-N rectangular matrix $U(n)$ using the covariance method of data windowing, where M is the filter order (here it is 15), and N is the length of each input vector:

$$U(n) = \begin{bmatrix} r(M) & r(M+1) & \dots & r(N) \\ r(M-1) & r(M) & \dots & r(N-1) \\ \dots & \dots & \dots & \dots \\ \dots & \dots & \dots & \dots \\ r(1) & r(2) & \dots & r(N-M+1) \end{bmatrix} \quad (4.17)$$

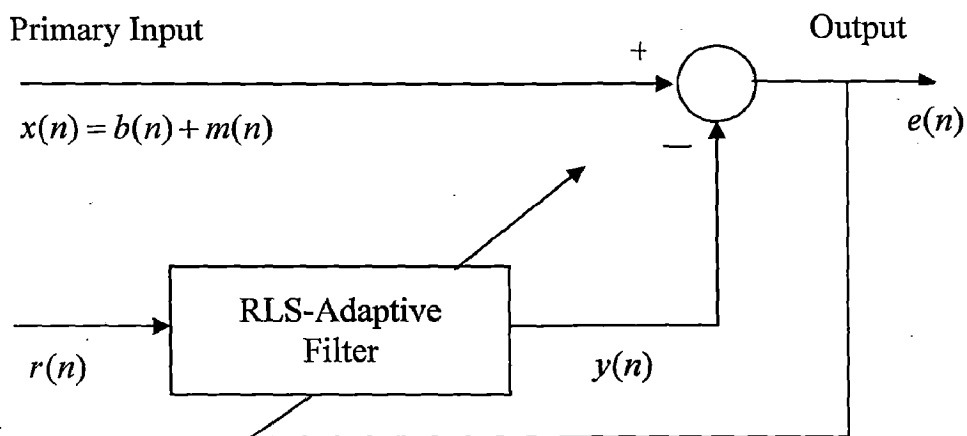


Fig.4.34 Block diagram of RLS-ANC filter

The algorithm serves to process the reference data $U(n)$ column-by-column and the primary signal $x(n)$ sample-by-sample, in order to estimate the tap weights W_k of the transversal filter such that the actual output of the RLS adaptive filter, $y(n)$, is as close to the interference component of the primary input as possible in the MSE sense. Likewise, the output of the ANC filter, $e(n)$, is the minimum MSE (MMSE) estimate, $g(n)$, of the information bearing component of the primary signal [15]:

$$g(n) = e(n) = x(n) - y(n) = ([b(n) + m(n)]) - y(n) \quad (4.18)$$

where

$$y(n) = \sum_{k=0}^{M-1} w_k r(n-k) = W^H(n)u(n) \quad (4.19)$$

$$\text{and } w(n) = w(n-1) + k(n)([x(n) - W^H(n-1)u(n)]) \quad (4.20)$$

in which, $w^H(n)$ is the Hermitian transposition of the tap weight vector calculated for the current iteration n , $u(n)$ is the n^{th} column of $U(n)$. Using 4.18, the MSE is determined as:

$$E[e^2(n)] = E[b^2(n)] + E[\{m(n) - y(n)\}^2] + 2E[b(n)\{m(n) - y(n)\}] \quad (4.21)$$

Since all signals in the third term of (4.21) have been filtered to remove DC and hence have zero mean, this term vanishes. Minimizing the remaining terms, the MMSE is shown as:

$$\min E[e^2(n)] = \min E[b^2(n)] + \min E[\{m(n) - y(n)\}^2] \quad (4.22)$$

Rearranging (4.18) as $e(n) - b(n) = m(n) - y(n)$, it is clear that both the RLS filter output $y(n)$ and the ANC output $e(n)$ are MMSE estimates of the interference $m(n)$ and the information-bearing component $b(n)$ of the primary input, respectively.

Elaborating on the operation of the RLS algorithm, for every $u(n)$, the Kalman gain, k , is determined

as:

$$k(n) = \frac{P(n-1)\lambda^{-1}u(n)}{(1 + u(n)^H P(n-1)\lambda^{-1}u(n))} \quad (4.23)$$

The matrix P is initialized as $P(0)=I\delta$, where I is the identity matrix, and δ is a regularization parameter, chosen as less than 0.01 times the variance of the primary input

The "forgetting factor", λ represents the memory of the algorithm, and for this study $\lambda = 1$, which implies infinite memory. The rest of the algorithm serves to update the P matrix, tap weights (initialized to zeros), and outputs $y(n)$ and $e(n)$ based on these values.

After using this RLS-ANC filter this estimated and desired output signal which is of having reduced heart sounds is as shown in figure 4.35.

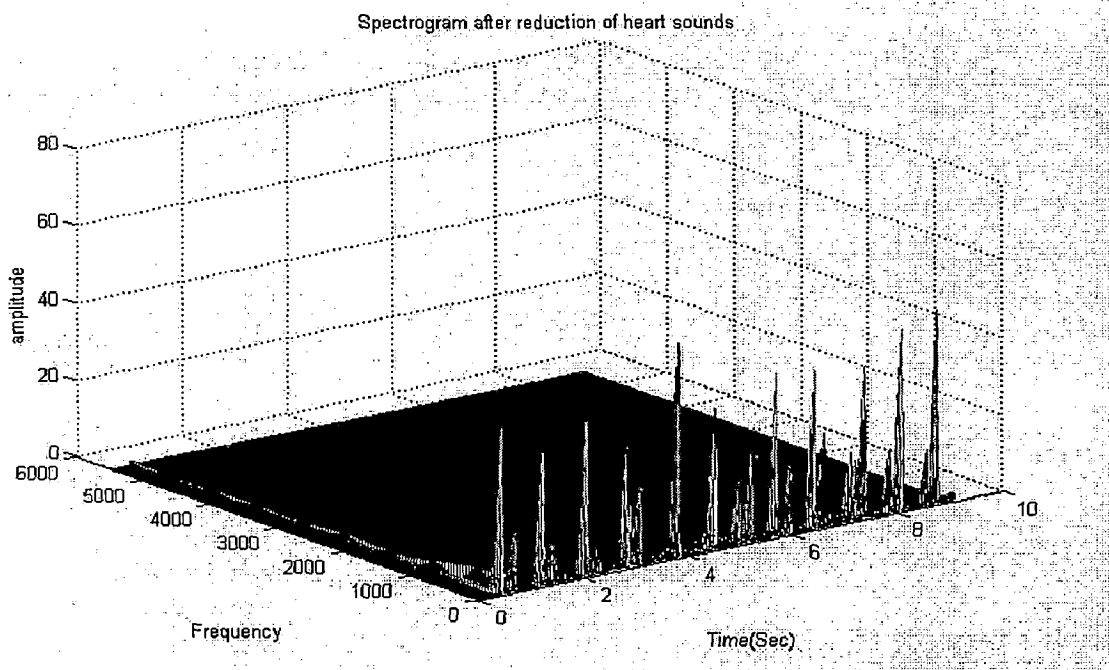


Fig.4.35 Spectrogram after reduction heart sounds

Sample2

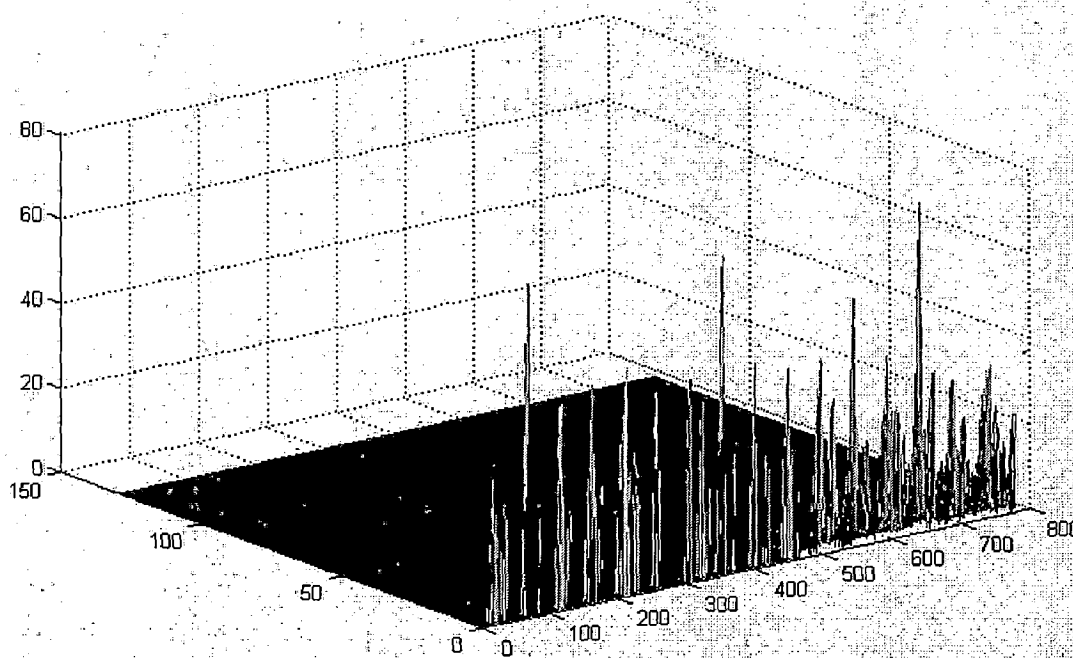


Fig.4.36 Spectrogram of lung sounds with heart sounds

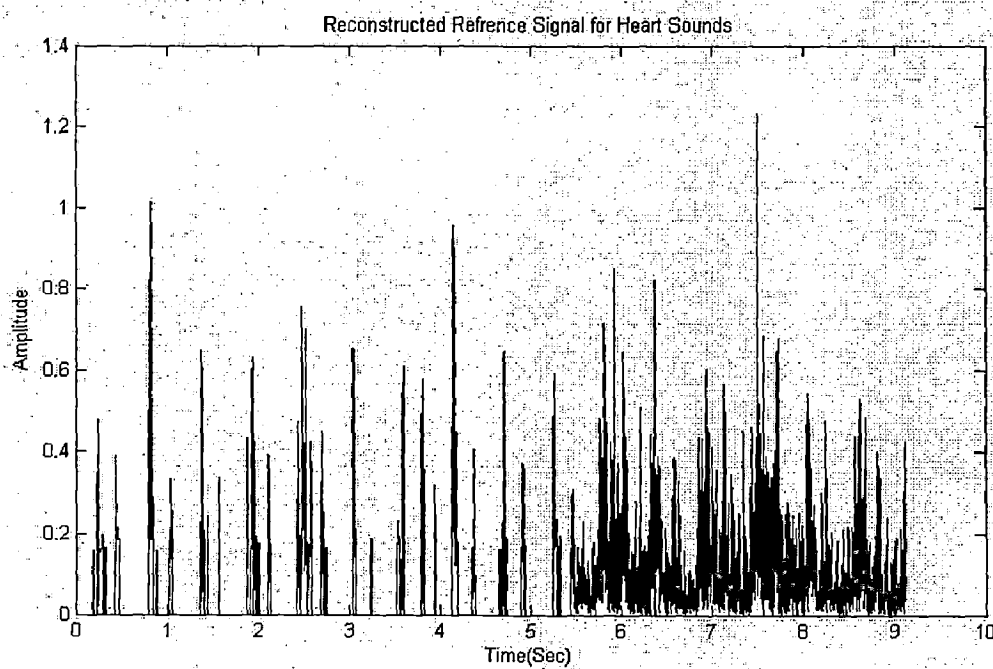


Fig.4.37 Reference signal for heart sounds

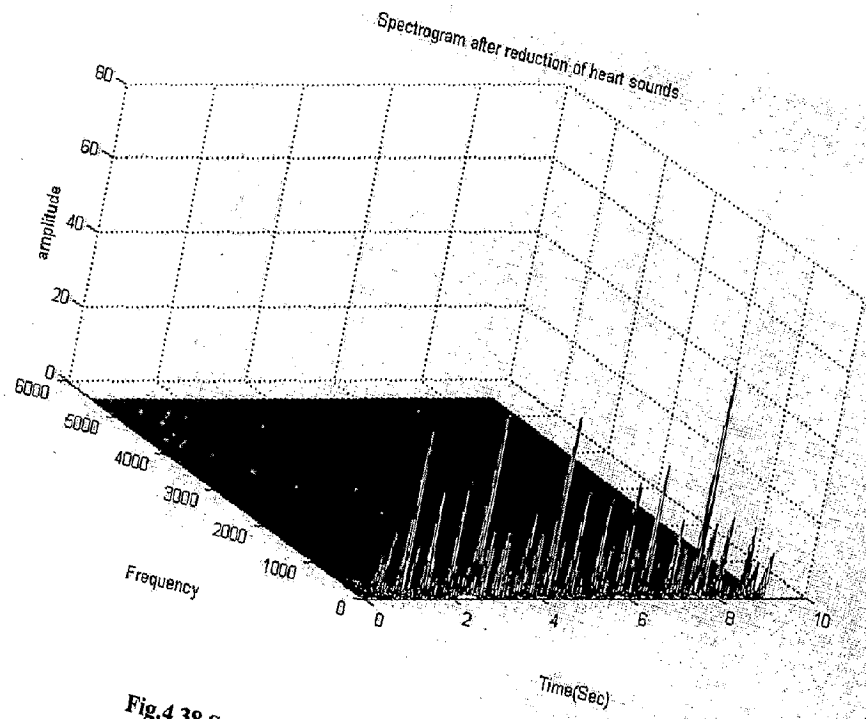


Fig.4.38 Spectrogram after reduction heart sounds

CHAPTER-5

CONCLUSIONS AND SCOPE FOR FUTURE WORK

In this work we used adaptive filters to remove adventitious sounds from normal breath sounds and by using time frequency analysis techniques some of the adventitious sounds are removed and original signal is reconstructed with out these adventitious sounds.

Conclusions:

- Hard ware Instrumentation is developed for acquiring Lung Sounds. This consists of sensing unit, amplifier and filter circuit .Output of this hard ware given to A/D converter and some low level I/O programming is done to record signal.
- Crackles (Rales) are adventitious sounds which non stationary in nature are removed from the lung sounds by using LMS (least mean square) adaptive filter which separates stationary signal from nonstationary signal. Initially coefficients of this filter are obtained by training the filter and after getting the coefficients this filter implemented over our desired signal.
- Wheezes are also nonstationary musical sounds which are of sinusoidal in shape. These generally occur at the time of expiration. We separated these wheeze episodes by decomposing original signal to frequency signal where these wheezes are dominant and there by applying threshold criteria. By using IDWT waveform is reconstructed.
- Lung sounds consists of various unwanted signals like heart sounds and respiratory muscle sounds. These heart sounds are of very low frequency compared to these lung sounds. In this work we localized these heart sounds by using spectrogram and reference signal for heart sounds is constructed. By using RLS (Recursive Least Square) adaptive filter and with help of this reference signal heart sounds are removed from original signal.

Scope for Future Work:

In this work we recorded signal from one channel but in case of lung sounds these are having various intensity levels at various locations on anterior and posterior of the chest so this work can be extended by multiple channels recording with very high sensitivity microphone with help of belt.

In case of wheeze removal one important factor to be mentioned is that these wheezes dominated in very high frequency range so we have to remove these wheezes in multiple levels when we are decomposing but at that time we are going to loose desired information. So this work is extended to remove complete wheeze episodes.

REFERENCES

- [1]. F. Schuttler, T. Penzel, P. von Wiichert, "Digital recording and computer based analysis of lung sounds," *Proc. IEEE on EMBS*, Vol-2, pp. 2301-2302, Nov.1996
- [2]. Kahya.Y.P, Cini.U, Cerid.O., "Real-time regional respiratory sound diagnosis instrument," *Proc. IEEE on EMBS*, Vol-4, pp. 3098-3101, Sep. 2003.
- [3]. A.R.A. Sovijärvi, J. Vanderschoot, J.E. Earis, "Standardization of computerized respiratory sound analysis," *JE Earis - Eur. Respir. Rev* 10, pp. 585-646, Feb. 2000.
- [4]. Gross, V. Penzel, T. Hadjileontiadis, L.Koehler, Vogelmeier.C. "Electronic auscultation based on wavelet transformation in clinical use," *Proc. IEEE on EMBS*, Vol-2, pp. 1531- 1532, Aug. 2002.
- [5]. B. Widrow, I. M. McCool, M. G. Larimore, and C. R. Johnson, Jr., "Stationary and nonstationary learning characteristics of the LMS adaptive filter," *Proc. IEEE*, vol-64, pp. 1151-1162, Aug. 1976.
- [6]. Welch.P, IBM Watson Research Center, Yorktown Heights, N.Y., "The use of fast Fourier transform for the estimation of power spectra: A method based on time averaging over short, modified periodograms," *IEEE Transactions on Audio and Electroacoustics*, Vol-15, pp. 70- 73, Jun.1967.
- [7]. Benedetto.G, Dalmasso.F, Spagnolo.R. "Surface distribution of crackling sounds," *IEEE Transactions on Biomedical Engineering*, Vol-35, pp. 406-412, May.1988.
- [8]. Du. M, Lam. F.K, Chan.F.H.Y, Sun. J., "Multi-resolution decomposition applied to crackle detection," *IEEE International Conference on Systems, Man, and Cybernetics, Florida, USA*, Vol-5, pp. 4223-4226, Oct.1997.

- [9].Du. M, Lam. F.K, Chan.F.H.Y, Sun. J., "Crackle detection and classification based on matched wavelet analysis," *Proc. IEEE on EMBS*, Vol-4, pp. 1638-1641, Nov.1997.
- [10].Mariko.O, Kaoru Arakawa, Masashi.M, Tsuneaki.S, Hiroshi.H., "Separation of fine crackles from vesicular sounds by a nonlinear digital filter," *IEEE Trans. on Biomedical Engineering*, Vol-36, pp. 286-291, Feb.1989.
- [11].Homs-Corbera.A, Jane.R, Fiz.J.A, Morera.J., "Algorithm for time-frequency detection and analysis of wheezes," *Proc. IEEE on EMBS*, Vol-4, pp. 2977-2980, Nov. 2000.
- [12].Homs-Corbera.A, Fiz.J.A, Morera.J, Jane.R., "Time-frequency detection and analysis of wheezes during forced exhalation," *IEEE Trans. on Biomedical Engineering*, Vol-51, pp. 182- 186, Jan. 2004.
- [13].Taplidou.S.A, Hadjileontiadis.L.J, Kitsas.I.K, Panoulas.K.I, Penzel.T, Gross.V., "On applying continuous wavelet transform in wheeze analysis," *Proc. IEEE on EMBS*, Vol-2, pp. 3832- 3835, Sept. 2004.
- [14].S. A. Taplidou, L. J. Hadjileontiadis, T. Penzel, V. Gross, and S. M. Panas, "WED: an efficient wheezing-episode detector based on breath sounds spectrogram analysis," *Proc. IEEE EMBS*, Vol-17, pp. 2531-2534, Sep. 2003.
- [15].Gnitecki.J, Moussavi.Z, Pasterkamp.H., "Recursive least squares adaptive noise cancellation filtering for heart sound reduction in lung sounds recordings," *Proc. IEEE on EMBS*, Vol-3, pp. 2416- 2419, Sept. 2003.
- [16].Pourazad.M.T, Mousavi.Z.K, Thomas.G., "Heart sound cancellation from lung sound recordings using adaptive threshold and 2D interpolation in time-frequency domain," *Proc. IEEE on EMBS*, Vol-3, pp. 2586- 2589 , Sept. 2003.

- [17].E. Saatci, A.Akan, "Heart sound reduction in lung sounds by spectrogram,"^{3rd}
European Medical and Biomedical Engineering Conference (EMBEC), Nov. 2005.
- [18].Emmanuel C. Ifeakor, Barrie W.Jervis., "Digital signal processing,"^{2nd} *Edition*,
Pearson Education, March. 2002.
- [19]. R.A.L.E. Respiratory. Available: <http://www.rale.ca/>
- [20]. <http://www.getbodysmart.com/ap/resp/resp.html>
- [21]. <http://www.le.ac.uk/pa/teach/va/anatomy/case2/frmst2.html>
- [22]. Matlab Wavelet Toolbox Manual.
- [23]. R.Polikar. 'The wavelet tutorial' (four parts)
<http://users.rowan.edu/~polikar/WAVELETS/WTtutorial.html>
- [24].Simon Haykin, "Communication systems," ^{2nd} *Edition*, *Wiley Eastern Limited*,
April.1983.

APPENDIX – I

1. Specifications of Microphone Used:

Frequency Response	50-16,000Hz
Sensitivity	3.5mV/Pa
Impedance	1000 Ω
Operates on	1 \times 1.5V (LR-44) Button Cell

2. ADC PCL-206:

2.1 Main Features of PCL-206:

Main features of PCL-206 high performance multifunction card are listed below for quick reference.

- 12 bit, 7 micro sec conversion time with MAX 162.
- 16 single ended or 8 differential channels selection.
- Fast and low drift instrumentation amplifier and sample/hold.
- Software, periodic and external, start conversion modes.
- DMA, interrupt and polling modes for data transfer.
- Higher and lower limits of the channels to be scanned can be programmed.
- 8 TTL input and 8 TTL output lines.
- 8254 timer/counter chip offering three channels.
- One counter/ timer channel available to user.
- Two channels cascaded for periodic A/D conversion generation. It has 8 MHz or 1 MHz clock or external clock as input.

2.2 Specifications of PCL 206:

- **Analog Input**

Primary Channels	:	8 differential or 16 single ended. (jumper selectable).
Resolution	:	12bits.
Input range	:	+/-5V, +/-10V and user available (jumper selectable)
Accuracy	:	0.01 % of reading +/- 1 bit
Over Voltage	:	Continuous 30 V max.
Conversion time	:	7 Microseconds.

- **TTL Output**

Channels	:	8 bits
Output		
Low voltage	:	0.5V maximum at Sink = 8mA.
High voltage	:	2.4V minimum at source = 4mA

- **TTL Input**

Channels	:	8 bits.
Input		
Low voltage	:	0.8V maximum
High voltage	:	2.4V minimum
Low current	:	0.4 mA maximum
High current	:	20 microamperes maximum at 2.7 V

- **Programmable Counter/ Timer**

Device	:	8254
Time base	:	0.8 MHz or 1 MHz jumper selectable.
Pacer output	:	71 minutes/pulse to 2 MHz

Counters : 3 channels! 16 bit 2 channels permanently connected to 8 MHz! 1 MHz clock as programmable pacer, 1 channel is free for user applications.

Time base : 8 MHz Or 1 MHz jumper selectable.

Pacer output : 71 minutes/ pulse to 2 MHz

- **Interrupt Channel**

Level : IRQ 2 to 7, software selectable.

Enable : Via control register.

- **DMA Channel**

Levels : 3 (Switch selectable).

Enable : Via control register.

User should initialize the appropriate 8237 DMA Channel. Each conversion raises DMA request two times. First lower byte is transferred and later higher byte with the channel number in MS nibble is supplied. This mode has to be enabled in the control register.

- **Power Consumption**

+5V : 1.35 Amp. (typical)

- **Mechanical Details**

Main connector: 20 pin FRC connector.

2.3 Base I/O Address Selection

PCL-206 occupies 16 consecutive I/O address locations. When selecting the I/O base address care should be taken that address do not overlap with other add-on cards. DIP switch (SW1) on PCL-206 allows the user to select appropriate address. This also facilitates putting more than one PCL-206 card in the system.

The IBM-PC decodes I/O addresses only upto 3FF hex. Hence I/O addresses from 400 hex to 7FF hex appear to overlap with 000 to 3FF hex addresses. This process is repeated for every 1K I/O address space. Therefore care should be taken while selecting Base Address of the add-on cards.

Following are the valid and typically free I/O addresses in the IBM-PC I/O address map.

SWITCH ON = 0 OFF = 1

SWITCHES SW 1-7, 1-8 UNUSED

Address Range		1-6	1-5	1-4	1-3	1-2	1-1
From	To	A9	A8	A7	A6	A5	A4
200H	20FH	1	0	0	0	0	0
220H	22FH	1	0	0	1	0	0
300H	30FH	1	1	0	0	0	0
320H	32FH	1	1	0	0	1	0

2.4 Connector Pin Assignment

Analog Input (single ended channel)

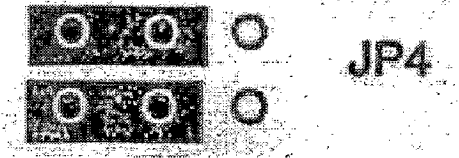
A/D S0	1	2	A/D S8
A/D S1	3	4	A/D S9
A/D S2	5	6	A/D S10
A/D S3	7	8	A/D S11
A/D S4	9	10	A/D S12
A/D S5	11	12	A/D S13
A/D S6	13	14	A/D S14
A/D S7	15	16	A/D S15
A.GND	17	18	A.GND
A.GND	19	20	A.GND

2.5 DMA Channel Selection

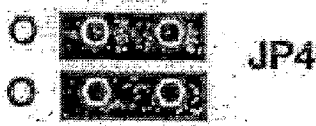
IBM-PC system devices and other special purpose cards in the system use certain interrupter DMA channels. DIP switch SW2 is used to select DMA channels in PCL-206 card. Select only those channels that are not used by the system.

JP4: Select Input Configuration

Select single ended inputs. (Refer JP6 - JPS)

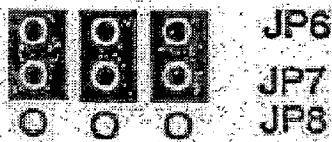


Select differential inputs (Refer JP6 - JP8)

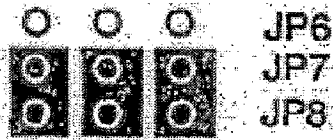


JP6 - JP8: Select Input Configuration

Select single ended inputs (Refer JP4)



Select differential inputs (Refer ~P4)



JP5: External Trigger Source Selection

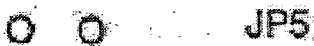
Select external trigger pulses

Through D10 input.



Select external trigger pulses

Through TRIGO input



JP9: Pacer Trigger Source Selection

Select 8 MHz source.



Select 1MHz source.



JP10: Counter 0 Gate Control Source

Counter 0 gate control through GATE 0 pin



Counter 0 gate control through DI2 pin.



2.6 Register Details for Software

2.6.1 General Register Format

PCL-206 occupies 16 consecutive I/O. addresses as given below (RD=Read, WR=Write).

[BASE+ 0]	RD	A/D Low Byte & Channel number.
	WR	Software A/D trigger.
[BASE+1]	RD	A/D High Byte.
	WR	N/A
[BASE+ 2]	RD	MUX scan channel.
	WR	MUX scan channel.
[BASE+ 3]	RD	Digital input.

	WR	Digital output.
[BASE+ 8]	RD	PCL-206status register.
	WR	Clear interrupt request.
[BASE+ 9]	RD	PCL-206control register
	WR	PCL-206control register
[BASE+10]	RD	N/A
	WR	Counter enable.
[BASE+ 12]	RD	Counter 0
	WR	Counter 0
[BASE+13]	RD	Counter 1
	WR	Counter 1
[BASE+14]	RD	Counter 2
	WR	Counter 2
[BASE+15]	RD	N/A
	WR	Counter control register

2.6.2 A/D Data Registers

The A/D data registers are read only registers with address BASE+0 and BASE+1. The AID channel number from which the conversion data was derived is available at BASE+ 0 lower nibble. The format in which the converted data and the channel number are available is given below.

[BASE + 0] Read Only.

D7	D6	D5	D4	D3	D2	D1	D0
AD3	AD2	AD1	AD0	CH3	CH2	CH1	CH0

[BASE + 1] Read Only.

D7	D6	D5	D4	D3	D2	D1	D0
AD11	AD10	AD9	AD8	AD7	AD6	AD5	AD4

2.6.3 MUX Channel Select

This register allows the user to specify the lower and the upper limits of channels to be scanned for A/D conversion. These can be either differential or single ended channels. Maximum channel number has to be according to the hardware jumper selection. (8 differential or 16 single ended). By performing write operation on this register, "data" of LOW CHANNEL LIMIT becomes the current channel. When the current channel becomes greater than the HI CHANNEL LIMIT, LOW CHANNEL LIMIT automatically gets loaded.

[BASE + 2] Read / Write.

D7	D6	D5	D4	D3	D2	D1	D0
CU3	CU2	CU1	CU0	CL3	CL2	CL1	CL0

Here "CU" stands for upper channel limit while "CL" stands for lower channel limit. This register can also be read back to check the channel limits.

2.6.4 Digital Output

Digital output section on this card consists of one independent 8 bit hardware port.

[BASE+3] Write only.

D7 D6 D5 D4 D3 D2 D1 D0

DO7 DO6 DO5 DO4 DO3 DO2 DO1 DO0

2.6.5 Digital Input

Digital input consists of one independent 8 bit hardware port. The input lines are scanned once during read operation.

Input I0 has capability of initiating A/D conversion, besides its role as simple input port line. To use it for triggering the A/D conversion jumper JP5 should be inserted and it needs low to high going edge. I2input can be used to control the operation of counter 0, besides its function as digital input. To connect I2 input to GATE of timer 0 jumper JP10

should be inserted in position 2-3. i.e.



[BASE+3] Read only.

D7 D6 D5 D4 D3 D2 D1 D0

DI7 DI6 DI5 DI4 DI3 DI2 DI1 DI0

Rest of the lines simply functions as digital input port lines.

2.6.6 A/D Status Register

This register provided on the board is very important since when read it gives feedback on the modes in which the card is presently being used. The format and the details are as follows.

[BASE+3] Read only.

D7	D6	D5	D4	D3	D2	D1	D0
BUSY	X	S/D	INT	CN3	CN2	CN1	CN0

BUSY: This bit gives the status of the A/D conversion.
BUSY=0 Conversion Over.
BUSY=1 ADC is busy.

X : This bit is always zero.

S/D : This bit indicates the single ended or differential mode of operation of the card.
S/D =0 8 Differential channels.
S/D =1 16 Single ended channels.

INT : Provides interrupt status.
INT=0 Interrupt disabled.
INT=1 Interrupt enabled.

CN3 to CN0: Next channel number waiting for conversion.
If BUSY=0, and ADC is triggered this channel would be immediately converted.

2.6.7 PCL-206 Control Register

This register enables user to select different modes and features of PCL-206 under program control. The modes can be set by writing this register. The modes set can also be read back by reading this register. The structure of this register is as follows.

[BASE+3]		Read / Write.			DON'T CARE = "X"		
D7	D6	D5	D4	D3	D2	D1	D0
INTE	IL2	IL1	IL0	X	DMAE	TR1	TR0

INTE : This particular bit controls the generation of interrupt. If this bit is set to "0" then interrupts are disable.

When this bit is set to "1" while setting DMAE=0, interrupt is generated following the End of Conversion.

When this bit is set to "1" with DMAE also set to "1", interrupt is generated. This interrupt is generated when T/C is received from DMA controller signifying that the DMA transfer is over.

IL2to ILO : Interrupt Level Selection.

By setting these three bits Interrupt level can be selected.

IL2	IL1	ILO	InterruptLevel
0	0	0	N/A
0	0	1	N/A
0	1	0	IRO2
0	1	1	IRO3
1	0	0	IRO4
1	0	1	IRO5
1	1	0	IRO6

1 1 1 IRO7

DMAE : This bit controls the DMA operation.
When DMAE= 0 DMA is disabled.
DMAE= 1 DMA is enabled.

TR1 and TR0 : Trigger Source Selection.

By setting these bits *ND* conversion trigger source can be selected.

TR1	TR0	Trigger Source
0	X	Software trigger
1	0	External trigger
1	1	Pacer trigger

2.6.8 Timer Enable Register

Two bits in this register control timer operation.

[BASE+10] Write only.

D7	D6	D5	D4	D3	D2	D1	D0
X	X	X	X	X	X	TC1	TC0

TC0 : Control of ADC triggering using timer.
TC0 =0 Pacer triggered enabled
TC0 =1 Pacer triggered disabled, until TRIG0 goes HIGH

TC1 : Counter 0 clock source selection.
TC1 =0 Configured to accept external clock pulses.
TC1 =1 Connects 100 KHz clock source internally.

2.6.9 Timer-Counter Control Register

PCL-206 uses 8254 timer-counter mainly for periodic triggering of A/D converter. The 8254 device is organized as independent counters. Counter 0 is totally user configurable. This counter can be used as a waveform generator. Counter 1 accepts either

8MHz or 1MHz clock input or output of Counter 1 forms input clock of Counter 2. Output of Counter 2 actually provides the triggering signal for A/D.

[BASE+12]	Counter 0 register	Read/ Write
[BASE+13]	Counter 1 register	Read/ Write
[BASE+14]	Counter 2 register	Read/ Write
[BASE+15]	8254 Control register	Read/ Write

2.7 Programmable Interval Timer/Counter

2.7.1 The 8254

PCL-206 uses the INTEL programmable interval timer / counter. The 8254 is a very popular timer / counter device consisting of three independent 16 bit down counters. Each counter has a clock input, control gate and an output. It can be programmed to have a count from 2 upto 65535.

The maximum clock input frequency is 10 MHz for the version 2 of 8254. PCL-206 provides 1 MHz and 8 MHz input frequency through an on-board crystal. The timer clock jumper JP9 is used for clock input rate selection.

The counter 1 and 2 are cascaded and operated in fixed divider configuration. Counter 1 input is connected to the 1 MHz or 8MHz input frequency and the output of the counter 1 is connected to the input of the Counter 2. The output of the Counter 2 is internally configured to provide trigger pulses to ND converter, but is also available for the PCL-206 for any internal use. User may access the counter 0 through Connector 5.

2.7.2 Counter Read/ Write and Control Registers

The 8254 programmable interval timer uses four registers at address BASE +12, 13, 14 and 15. The function of each register is:

BASE+12	Counter 0 Read/Write'
BASE+13	Counter 1 Read/Write
BASE+14'	Counter 2 Read/Write
BASE+15	Counter Control Word

The data format of the *control register* is:

[BASE+15]

D7	D6	D5	D4	D3	D2	D1	D0
SC1	SC0	RW1	RW0	M2	M1	M0	BCD

SC1 & SC0 : Select Counter.

SC1	SC0	Counter
0	0	0
0	1	1
1	0	2
1	1	Read-back command

RW1 & RW0 : Select the Read/ Write operation

RW1	RW0	Operation
0	0	Counter latch
0	1	Read/ Write LSB
1	0	Read/ Write MSB
1	0	Read/ Write LSB first, then MSB

M2, M1 and M0 : Select the Operating Mode.

M2	M1	M0	MODE
0	0	0	0 – Interrupt on terminal count
0	0	1	1 – Programmable one shot
X	1	0	2 -Rate generator
X	1	1	3 - Square wave rate generator
1	0	0	4 –Software triggered strobe
1	0	1	5 – Hardware triggered strobe IRO5

BCD -Select Binary or BCD Counting

BCD	Type
0	Binary Counter 16-Bits
1	Binary Coded Decimal (BCD) Counter (4 Decades)